SOVIET PHYSICS USPEKHI VOLUME 14, NUMBER 4 JANUARY-FEBRUARY 1972

539.186.3

INTERFERENCE PHENOMENA IN ATOMIC SCATTERING

E. E. NIKITIN and M. Ya. OVCHINNIKOVA

Usp. Fiz. Nauk 104, 379–412 (July, 1971)

TABLE OF CONTENTS

1. INTRODUCTION

FOR a long time, study of atomic collisions has been restricted to elucidating the fundamental features and mechanisms of elastic and inelastic processes, such as transport phenomena, charge transfer, excitation, and ionization. The task of the theory has consisted mainly in calculating the total cross-section from known (or assumed) potentials, and in calculating the kinetic coefficients of processes of physical and chemical kinetics. Attempts to interpret the macroscopic quantities in terms of molecular constants have always encountered the difficulty that many details of the interaction were obliterated in the averaging process. Thus it has proved practically impossible, and often even unnecessary, to give a microscopic description of the collision process.

As the technique of physical experimentation has developed, the necessity arose of describing the processes more exactly: of fixing the initial and final states of the colliding particles. New experimental methods (kinetic spectroscopy, crossed and overtaking molecular beams, analysis and separation of colliding particles with respect to their states in strong electric and magnetic fields, and selective excitation of states with a laser beam) have stimulated development of the theory of collisions in the low-energy range, from fractions to thousands of electron volts. Many unsolved problems have arisen unexpectedly, even in well-developed fields, e.g., such as the elastic scattering of heavy particles. Fundamentally, these problems arose in connection with the possibility that has arisen of "unfolding" many processes in terms of energy and scattering angle. These unfoldings, which are the differential cross-sections for inelastic scattering at different kinetic energies, and with given quantum states of the particles, are reminiscent of spectrograms. Their structure contains a mass of information on the fine details of the mechanism of the process. To obtain such information and to interpret it already constitutes an entire field in the physics of atomic collisions, and it is commonly called collision spectroscopy.

Study of collisions of electrons with atoms and molecules (electronic collision spectroscopy) at low energies has made it possible to discover a number of new resonance phenomena. When supplemented by information about the angular distribution of the electrons, the energy characteristics of the resonances then give information on the quasistationary states of molecules that suffices for constructing models of the multielectron systems. Consequently, the problem of the theory of scattering of electrons by molecules have proved to be closely related with those of the theory of the electronic structure of molecules, which traditionally belong to quantum chemistry.

An even closer merger of physics and chemistry appears in the field of atomic and molecular collision spectroscopy, in particular, in studying very simple chemical reactions in molecular beams. The significance of these studies for applications is evident. However, the difficulties that one generally encounters along this line, both experimental and theoretical, are very large. Among the entire set of collision problems, only one (atomic collision spectroscopy) is in such a state that the vast experimental material can be classified and discussed from a single viewpoint. This is exactly why we shall restrict ourselves to treating only atomic collisions, with the hope that the presented methods will prove useful also in other fields of collision spectroscopy.

In line with this, the task of the theory is to interpret the experimentally observed complex structure of the cross-sections, and to obtain the quantitative characteristics of the interaction potentials of the particles from the scattering data. The energy terms (potentials) of a colliding pair can be obtained in two ways. The first is a non-empirical (ab initio) calculation of the properties of the molecular electronic states as a function of the internuclear distances, with subsequent solution of the problem for comparison of the predicted and observed cross-sections. These calculations are very laborious and expensive, so that the number of systems amenable to such a study is as yet very restricted. Hence, together with the first approach, a second approach in the theory in this field seems very valuable, namely, to develop general principles and the most general models for the characteristic types of interactions. On the basis of the latter, we can interpret the experimental data and derive from them the specific parameters of the interatomic interactions.

This review will treat the fundamental methods of the second approach in particular, to which too little attention has been paid in the recently published books on collisions.[1-6] We should note the recently

published reviews[7-12] on analogous topics. As compared with[7-12], we shall allot more attention in our review to the theory of inelastic processes, obligatory pseudo-crossings, and threshold phenomena related to them.

Our presentation begins with general methods of describing elastic and inelastic processes at energies and scattering angles such that the potential can be treated in a certain sense as a perturbation (Chap. 2). This so-called "high-energy" approximation proves to be applicable even for relatively slow-collisions. In this regard, we shall make it the basis of the subsequent discussion, since this is precisely the case in which one can get the most reliable experimental data and handle them in the simplest form. Then we shall treat interference phenomena in the elastic scattering of atoms having a typical interaction potential (attraction at large distances and repulsion at small distances) (Chap. 3). These phenomena are due to addition of amplitudes of de Broglie waves scattered at the same angle by different regions of the potential. It turns out that one can draw an analogy here, first, with many optical phenomena in the atmosphere (halos, rainbows), and second, with certain interference phenomena in inelastic processes. The first point involves the fact that the wavelength of the particles and the parameters of the potential are related qualitatively in a way that permits an analogy with the relation between the wavelength of light and the parameters of droplets. The second analogy is based on the fact that scattering of waves by different regions of a potential in a certain sense resembles scattering of a wave by different potentials between which there is a more or less localized coupling.

Then we shall discuss resonance processes (Chap. 4), for which there is no coupling between the adiabatic potentials, and the inelastic process is described by interference of two independent waves. Each of these waves in turn now carries memory of the structure of the corresponding potential.

Finally, we shall discuss inelastic processes with a localized coupling between terms (Chap. 5), i.e., the case in which the non-adiabatic interaction between different energy states proves to be localized within relatively narrow ranges of variation of the internuclear distance. In this situation, in order to find the scattering matrix, it suffices to solve the problem of non-adiabatic transitions in these regions alone, and to link this solution with the adiabatic (transitionless) quasiclassical solution outside these small regions. It is precisely this circumstance that permits us in many cases to avoid solving the quantum problem of multichannel scattering.

The last part of the review will be devoted to the theory of anomalies in differential cross-sections near the threshold of an inelastic process. Here we should make the reservation that we take "threshold" phenomena to mean phenomena at energies and scattering angles near to the experimental threshold of an inelastic process. Under conditions of classical atomic collisions, this means that a large number of partial waves contribute to the cross-section of the process in the region of interest to us near the threshold. This is to be distinguished from threshold and resonance phenomena in nuclear physics, which are usually determined by the behavior of a single partial wave alone.

The fact that the conditions of quasiclassical collisions can be satisfied has determined the methodological style of presentation: we have attempted in all possible cases to describe the interference phenomena in terms of quantities associated with motion along classical trajectories. Such an approach simplifies comparison of the quantum theory with the classical, which is currently widely used in molecular collision spectroscopy. The cited experimental data are adduced only to illustrate the overall situation, and make no pretense at completeness.

2. CHARACTERISTIC PARAMETERS AND GENERAL FORMULATION OF THE PROBLEM OF ATOM SCATTERING AT LARGE ENERGIES

In classical mechanics, the deflection angle χ of the trajectory of a particle in a potential field U(R) as a function of the impact parameter b and the energy E of the system is determined by the well-known equation

$$\frac{1}{2}[\pi-\chi(b,E)]=\int_{R_0}^{\infty}\frac{BdR}{R^2\left(1-\frac{U}{E}-\frac{b^2}{R^2}\right)^{1/2}}, \qquad (1)$$

Here R_0 is the turning point of radial motion, which is the largest root of the radicand in (1). Figure 1a shows a typical form of the function $\chi(b)$. In distinction from the deflection angle $\chi(b)$, which changes sign as a function of the sign of the potential (positive for repulsion, negative for attraction), the observed scattering angle θ, which by definition is measured in the interval $(0, \pi)$, is

$$\theta=\min|\chi-2\pi n| \qquad (2)$$

and it is shown in Fig. 1b. In general, the inverse relation $b = b(\theta)$ of the impact parameter to the scattering angle is multivalued. For example, the single scattering angle θ' in Fig. 1b corresponds to three different trajectories having impact parameters b_1, b_2, and b_3. Correspondingly, the classical cross-section equals the sum of contributions of all branches of the scattering at the angle θ:

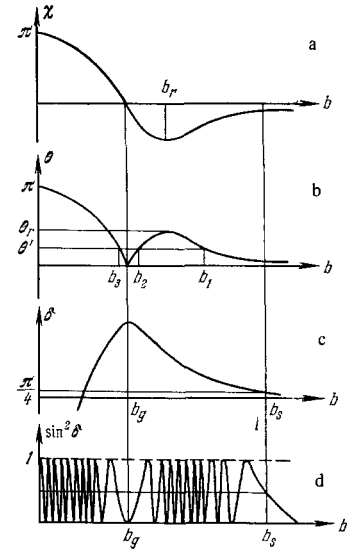

FIG. 1. Typical relations of: a) the deflection angle χ; b) the scattering angle θ; c) the phase δ; d) $\sin^2\delta$, as functions of the impact parameter b for an interatomic potential having a minimum. The subscripts 1, 2, and 3 indicate the different branches of the function $b(\theta)$.

$$\sigma(\theta) = \sum_i \sigma_i(\theta) = \sum_i \frac{1}{\sin\theta} b_i \left|\frac{db_i}{d\theta}\right|. \quad (3)$$

Equation (3) assumes that the contributions from different branches of the function $b = b(\theta)$ are independent. However, when one examines the scattering in more detail, even in purely elastic scattering, the possibility arises immediately of quantum interference of the contributions from different trajectories. This leads to a complex oscillatory structure of the cross-section. The problem is complicated by the fact that the theory of inelastic scattering accompanied by excitation of the atoms, charge transfer, etc., does not reduce to the theory of potential scattering of structureless particles. Rather, it includes also the theory of electronic transitions upon collision of heavy (atomic) particles.

The overall formulation of the problem of elastic and inelastic atomic scattering is well known.[13]

In the simplest semiclassical formulation of the problem, the wave function of the system is expanded over a certain complete set of electronic functions φ_n:

$$\Psi(\mathbf{r}, t) = \sum_n c_n(t)\varphi_n(\mathbf{r}, R(t)), \quad (4)$$

while the motion of the nuclei is considered to proceed over a single classical trajectory $\mathbf{R} = \mathbf{R}(t)$, which corresponds to some potential averaged over the electronic states.

The variation in the coefficients $c_n(t)$ is determined by the Schrödinger equation

$$i\hbar \frac{dc_n}{dt} = \sum_m [U_{nm}(\mathbf{R}) + \dot{\mathbf{R}}\mathbf{P}_{nm}] c_m(t), \quad (5)$$

where $U_{nm} = \langle \varphi_n | \hat{H}_{el} | \varphi_m \rangle$ is the potential-energy matrix, and $\mathbf{P}_{nm} = -i\hbar \langle \varphi_n | \partial/\partial \mathbf{R} | \varphi_m \rangle$ is the matrix of the non-adiabaticity operator. The conditions for $t = \pm\infty$ determine the initial state and the result of collision.

In principle, it suffices to know the matrices U_{nm} and $\mathbf{P}_{nm}$ to solve the problem for any basis φ_n. However, in order to get concrete results, one usually limits the treatment to a finite and often very small set of functions φ_n. This is precisely the stage at which the problem arises of correct choice of a basis that minimizes the errors involved in omission of the infinite set of states.

One of the important special cases is an adiabatic basis, in which the φ_n are defined as the eigenfunctions of the Hamiltonian $\hat{H}_{el}$ for fixed R. The physical argument for choosing this basis[13] is based on the possibility of approximate separation of nuclear and electronic motion (the adiabatic approximation). Since the velocities of the atoms (even at energies $E \approx 10^3$ eV) are small in comparison with the velocities of electronic motion, the state of the electrons can adjust to a given position of the nuclei.

On this basis, the potential matrix U_{nm} is diagonal, and the mean electronic energy U_n in the state n (the electronic term) plays the role of the potential energy for adiabatic motion of the nuclei. The electronic states are coupled only by the non-adiabaticity operator (the second term in square brackets in (5)). Here the order of magnitude of the probability of a transition between two electronic states is determined by the non-adiabaticity parameter or the Massey parameter

$$\xi = \omega\tau = \frac{\Delta U_{min}}{\hbar}\frac{\Delta R}{v}, \quad (6)$$

which equals the product of the characteristic frequency $\omega = \min(U_{nn} - U_{mm})/\hbar$ of the transition by the time τ for passage through the non-adiabaticity region.

For values $\xi > 1$, the transition probability is exponentially small ($\sim\exp(-2\pi\xi)$). Consequently, in fact, the electronic transitions occur in relatively narrow ranges ($\Delta R \ll a_0$) in which the adiabatic terms approach, or in regions where the functions of the adiabatic basis become rearranged (for different types and models of non-adiabatic transitions, see[14,15]). A typical situation of such an approach (quasi-crossing) occurs when the terms $U^0_{11}(R)$ and $U^0_{22}(R)$ calculated in some crude approximation (neglecting the interaction component) intersect at the point R_p. Only when we take into account the omitted interaction U^0_{12} do the adiabatic terms shift apart by the amount $2|U^0_{12}|$, where U^0_{12} is the matrix element of interaction between the states 1 and 2 of the chosen basis. In this case, the functions of the truly adiabatic basis (the eigenfunctions of the complete Hamiltonian $\hat{H}_{el}$) are related at the intersection point only by a differential coupling. In the region of intersection it has a maximum value of $\hbar v/\Delta R$, where v is the velocity of the nuclei, and the dimension ΔR of the transition region can be estimated to be

$$\Delta R \approx |U^0_{12}(R_p)| \Big/ \frac{d}{dR}(U^0_{11} - U^0_{22})_{R=R_p}. \quad (7)$$

Another basis that is opposite to the adiabatic basis is the so-called "diabatic" basis φ'_n, which lacks the differential non-adiabatic coupling $\mathbf{P}'_{nm} = \langle \varphi'_m(-ih\frac{\partial}{\partial R})\varphi'_n \rangle = 0$, while the entire coupling is effected by the potential-energy matrix U'_{nm}.

One can construct such a basis from the adiabatic basis[17] if one knows the matrix $\mathbf{P}_{nm}$ in the adiabatic basis and if one assumes that $\mathbf{P}_{nm} \to 0$ as $R \to \infty$. However, there is a difficulty that amounts to the fact that the matrix $\mathbf{P}_{nm}$ does not vanish as $R \to \infty$, but is of the order of magnitude of $\hbar v/a_0$ (a_0 is the atomic dimension). This is because the adiabatic functions do not give a correct asymptotic form for the separating atoms. Hence, one can construct a diabatic basis from the adiabatic basis only to an accuracy of terms in $\hbar v/a_0$. The latter are not substantial in comparison with the maximum value $hv/\Delta R$ of the non-adiabatic coupling in the transition region only under the condition that the dimensions of this region are small: $\Delta R \ll a_0$. One can eliminate this difficulty partially by using an expansion over non-orthogonal moving atomic orbitals.[18,19]

Figure 2 shows a typical form of the terms in a quasi-crossing region on diabatic and adiabatic bases. A study of an exactly-solvable model (see Chap. 5, the Landau-Zener model) of such a quasi-crossing implies that the system follows the adiabatic terms at low velocities with a probability close to unity. However, at high velocities the motion follows the smoothed diabatic terms (see Fig. 2). This is just why the diabatic potential curves and the functions derived in the independent-particle approximation (i.e., in the molec-

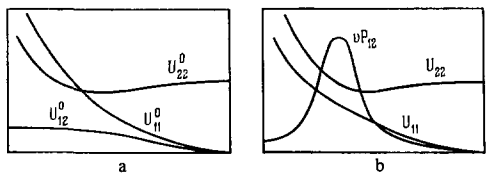

FIG. 2. Coupling of electronic terms on the diabatic and adiabatic bases. a) Elements of the potential matrix on the diabatic basis; b) the terms and the matrix element of the non-adiabaticity operator on the adiabatic basis.

ular-orbital approximation) without account of the correlation energy of the electrons play a large role in interpreting scattering phenomena at high energies.[16,20]

Let us proceed to discuss the collision problem, bearing in mind mainly high-energy scattering at small angles.

In the semiclassical treatment, this means that the mean classical trajectory of motion of the atoms closely approximates a linear trajectory:

$$R(t) = [b^2 + v^2 t^2]^{1/2}, \tag{8}$$

where b is the impact parameter, v is the velocity of the atoms, which is independent of the electronic state of the system at high energies ($E \gg U_n - U_m$). The transition probability $P_{nm}(b)$ as a function of the impact parameter is found by solving the equations (5) with the trajectory R(t) from (8). Here the small scattering angle θ corresponding to a given b is determined from the formula for classical scattering in a certain mean potential $\bar{U}(R)$:

$$\theta = \left| \frac{1}{2E} \int_{-\infty}^{\infty} \frac{b}{R} \frac{d\bar{U}}{dR}\, dz \right|, \quad R^2 = b^2 + z^2. \tag{9}$$

Equation (9) is a special limiting case of Eq. (1) for large energies for which

$$E \gg \bar{U}(R). \tag{10}$$

Now we shall use this condition for a quasiclassical formulation of the problem of inelastic scattering at small angles (the so-called high-energy approximation;[21,22] for an overall formulation, see[13,23]). The Hamiltonian of the system equals the sum of the kinetic energy of the nuclei and the electronic Hamiltonian:

$$H = -\frac{\hbar^2}{2\mu} \Delta_R + H_{el}(\mathbf{r}, \mathbf{R}). \tag{11}$$

At large energies, the interaction of the atoms is treated as a perturbation that slowly modulates the incident wave. Correspondingly, the wave function of the system can be sought in the form

$$\Psi(\mathbf{r}, \mathbf{R}) = \sum_n A_n(\mathbf{R})\, e^{ik_n z} \varphi_n^0(\mathbf{r}, \mathbf{R}), \tag{12}$$

where $A_n(R)$ is a function that varies slowly in comparison with $\exp(ik_n z)$. If we substitute (12) into the Schrödinger equation and omit the second derivatives of the functions A_n with respect to R (the condition of slow modulation), we get equations for the amplitudes A_n:

$$i \frac{\hbar^2 k_n}{\mu} \frac{\partial A_n}{\partial z} + \sum_m U_{nm} A_m + \sum_m i \frac{\hbar^2 k_m}{\mu} \left\langle \varphi_n^0 \left| \frac{\partial}{\partial z} \right| \varphi_m^0 \right\rangle A_m = 0. \tag{13}$$

We can easily see that the equations (13) coincide with the parametric equations (5) with the rectilinear trajectory of (8) with the substitution z = vt. Here $v = \hbar k/\mu$ is the velocity of the atoms, which is independent of the level n at large energies ($E \gg U_n - U_m$).

The equations (13) must be integrated under boundary conditions that ensure the presence of only one electronic state $\varphi_{n_0}^0$ in the incident ($z \to -\infty$) wave: $\lim_{z \to -\infty} A(x, y, z) = \delta_{nn_0}$. Let us denote the amplitudes defined under these conditions as $A_{nn_0}(x, y, z)$. In particular, for elastic scattering in a potential U(r) (a one-electron state), integration of (13) gives (the subscript n_0 is omitted):

$$A(x, y, z) = \exp\left\{ -\frac{i}{\hbar v} \int_{-\infty}^{z} U(x, y, z)\, dz \right\}. \tag{14}$$

We can easily find from the form (12) of the wave function the amplitude $f_n(\theta)$ of scattering by the system at the small angle θ ($\theta \ll 1$) in a given electronic state φ_n^0. To do this, it suffices to take the corresponding Fourier component having momentum $\mathbf{k}' = \mathbf{k} + \mathbf{q}$ ($q = k\theta$) from the projection of the function

$$\Psi(\mathbf{r}, \mathbf{R}) - e^{+ikz} \varphi_{n_0}^0(\mathbf{r}, \mathbf{R})$$

onto the electronic state $\varphi_n^0(\mathbf{r}, \mathbf{R})$ that we are interested in. Thus we get[22] the following expression for the scattering amplitude:

$$f_n(\theta) = -2\pi i k_n \int_0^{\infty} b\, db\, [A_{nn_0}(b) - \delta_{nn_0}]\, J_0(k_n b\theta), \tag{15}$$

Here J_0 is a Bessel function, and the amplitudes $A_{nn_0}(b)$, which are equal to

$$A_{nn_0}(b) = \lim_{z \to \infty} A_{nn_0}(x, y, z), \quad b = [x^2 + y^2]^{1/2}, \tag{16}$$

are found by solving (13) with the initial conditions $A_n(x, y, z \to -\infty) = \delta_{nn_0}$. For potentials that decline faster than 1/R, the amplitudes A_{nn_0} differ from zero, and they oscillate rapidly (see[14]) for $b \le b_s$ and they decline rapidly for $b > b_s$. Here we can estimate the characteristic dimension b_s from the relation

$$\frac{1}{\hbar v} \int_{-\infty}^{\infty} U(b_s, z)\, dz \equiv 2\delta(b_s) \approx 1. \tag{17}$$

The expression (15) describes both quantum scattering (diffraction) at small angles for which $kb_s\theta \le 1$, and classical scattering at values of θ such that $kb_s\theta \gg 1$. In the latter case, if we use the asymptotic expansion of $J_0(x)$ for $x \gg 1$, we get the final expression for the scattering amplitude at high energies at small ($\theta \ll 1$) but classical ($kb_s\theta \gg 1$) scattering angles:

$$f_n(\theta) = \sqrt{\frac{2\pi k}{\theta}} \int_0^{\infty} \sqrt{b}\, db\, [A_{nn_0}(b) - \delta_{nn_0}]\, [e^{ikb\theta + i\frac{\pi}{4}} - e^{-ikb\theta - i\frac{\pi}{4}}]. \tag{18}$$

In the very simple case of purely elastic scattering in a potential U(R), the amplitude is, according to (14):

$$A(b) = \exp[2i\delta(b)],$$

where the phase is

$$\delta(b) = -\frac{1}{2\hbar v} \int_{-\infty}^{\infty} U(R)\, dz. \tag{19}$$

If we take account of the rapid oscillation of the inte-

grand in (18), we can easily relate the scattering amplitude $f_n(\theta)$ with the quantities that characterize the classical trajectories of motion in the potential U(R) (see the next chapter). However, even in simple potential scattering, the cross-section cannot always be reduced to the classical form (3). This is because interference has the result that the measureable quantities prove to be not only the moduli, but also the phases (19) of the scattering amplitudes. The rest of this review will be concerned with discussing the experimentally observed effects due to this interference, and with interpreting them.

In concluding this chapter, we note that the approximation discussed here, which is often called the "impact-parameter approximation" is a very simple variant of the so-called "eikonal approximation," or three-dimensional quasiclassical treatment, which has been developed recently in a number of studies[24-26] as applied to atomic collisions.

3. INTERFERENCE PHENOMENA IN ELASTIC SCATTERING

Phenomena of elastic scattering of atoms are explained to a considerable extent by classical mechanics. However, a number of important features of scattering require a quantum-mechanical interpretation. Discussion of these phenomena at high energies, in particular, is the topic of this chapter.

Let us trace the relation between the quantum and classical descriptions of elastic scattering.

The quantum-mechanical formula for the scattering cross-section is well known:

$$\sigma(\theta) = |f(\theta)|^2,$$

$$f(\theta) = \frac{1}{2ik}\sum_{l=0}(2l+1)(e^{2i\delta_l}-1)P_l(\cos\theta), \qquad (20)$$

Here $k = (1/\hbar)\sqrt{2\mu E}$, δ_l is the phase of the scattering in the lth partial wave, and P_l is the Legendre polynomial. Under conditions of atomic scattering, a great number of waves ($l \leq l_S \gg 1$) contribute to the scattering amplitude $f(\theta)$. Also, the phase δ_l of the scattering, for which we can use a quasiclassical expression, is a smooth function of l. Hence, the summation in (20) can be replaced by integration over l or over the impact parameter $b = \lambda\!\!\!^{-}(l + \frac{1}{2})$. Also, in the region of angles that are not too small: $\theta > 1/l_S = \lambda\!\!\!^{-}/b_S$ (see the discussion of (17) in Chap. 2), we can replace the polynomials P_l by their quasiclassical expression:

$$P_l(\cos\theta) = \left[\frac{1}{2}\left(l+\frac{1}{2}\right)\pi\sin\theta\right]^{-1/2}\sin\left[\left(l+\frac{1}{2}\right)\theta+\frac{\pi}{4}\right].$$

Thus we get the well-known[27,22] formula for the quasiclassical scattering amplitude:

$$f(\theta) = -\sqrt{\frac{2\pi k}{\sin\theta}}\int_0^\infty \sqrt{b}\,db\,\{e^{iS^+(b,\theta,E)} - e^{iS^-(b,\theta,E)}\}, \qquad (21)$$

Here the action $S^\pm(b, \theta, E)$ can be represented as a sum of radial and angular components:

$$S^\pm(b,\theta,E) = 2\delta(b,E) \pm kb\theta \pm \frac{\pi}{4}. \qquad (22)$$

The radial component $2\delta(b, E)$ is the quasiclassical limit of the quantum phase $2\delta_l$ for $l \gg 1$, and it equals the difference of radial actions for motion with and without the potential U(R):

$$\delta(b,E) = \lim_{R\to\infty} k\left\{\int_{R_0}^{R}\sqrt{1-\frac{U}{E}-\frac{b^2}{R^2}}\,dR - \int_b^R\sqrt{1-\frac{b^2}{R^2}}\,dR\right\}. \qquad (23)$$

In order to relate (21)–(23) to the classical scattering formulas (1)–(3), we must take into account the fact that the integrand in (21) is a rapidly oscillating function. Therefore, only neighborhoods of the stationary-phase points b_i contribute to the amplitude of (21). For these points, the rate of variation of phase vanishes:

$$\left|\lambda\frac{\partial 2\delta(b,E)}{\partial b}\right|_{b=b_i} = \theta, \quad \mathrm{mod}\,2\pi. \qquad (24)$$

We can easily convince ourselves that this relation coincides with the definition of the classical scattering angle in terms of the deflection angle χ.

Summation of all the contributions to the scattering amplitudes from the neighborhoods of the possible points b_i gives the expression for the scattering cross-section

$$\sigma(\theta,E) = |f(\theta)|^2 = \left|\sum_k \sigma_k^{1/2}(\theta,E)\,e^{iS_k[b_k(\theta,E),\theta,E]+i\gamma_k}\right|^2, \qquad (25)$$

Here $\sigma_i(\theta, E)$ are the classical contributions of the different branches to the total cross-section, and the $S_k(\theta, E)$ are the quasiclassical actions over the corresponding classical trajectories. The phase constants γ_i that arise upon summing the amplitudes over the small region Δb_i near $b_i(\theta, E)$ depend on the sign of $db_i/d\theta$. Here the quantities Δb_i, which are the dimensions of the regions that are essential in the integration in (21), are of the order of: $\Delta b_i \approx (\lambda\!\!\!^{-}b)^{1/2}/\theta^{1/2}$. Figure 3 shows the relation between $\sigma(\theta, E)$ and the functions $\sigma_k(\theta)$, $b_k(\theta)$, and $S_k(\theta)$.

Thus, even in simple potential scattering, quantum interference can occur between the fluxes that arise from classical trajectories that have different impact parameters, but which are scattered at the same angle θ. Here, according to (23) and (24), the action $S(b, \theta, E)$ not only serves as the generator of the deflection function $\theta(b)$ or its inverse function $b_i(\theta)$, but it also determines the observable fine structure of the scattering when interference exists in (25).

The quasiclassical approximation (25) cannot be applied whenever the actions or action differences are so small that the Δb_i become comparable to the b_i (small-angle scattering), or whenever two regions of Δb_i begin to overlap (scattering near an extremal deflection angle θ_r, or rainbow scattering). These angular regions, which are marked in Fig. 3c, must be treated in more detail, with account taken of the overlap of different regions of Δb_i that contribute to scattering at the same angle θ.

As is well known,[7] the final value of the total cross-section

$$q(E) = \int|f(\theta)|^2\,d\Omega = 2\pi\int_0^\infty b\,db\,|e^{2i\delta(b)}-1|^2 = 8\pi\int_0^\infty b\,db\sin^2\delta(b) \qquad (26)$$

is ultimately due to interference of the wave scattered at a small angle [the amplitude $e^{2i\delta(b)}$ in (26)] with the unscattered wave [the amplitude 1 in (26)]. If the potential declines rapidly enough, then a rough estimate of $q(E)$ can be obtained by the random-phase approximation.[13] It replaces the scattering by the true potential by the scattering by an equivalent rigid sphere of radius b_S (see (17)), or by the Landau-Lifshitz-

Schiff approximation,[7] which takes correct account of the diffuse edge of the scattering boundary. The first of these corresponds to averaging $\exp(2i\delta(b))$ for $b < b_S$, where this function oscillates rapidly, and replacing $\exp(2i\delta(b))$ by unity when $b > b_S$, where the phase is small. These approximations qualitatively correctly describe the interference effects in region I in Fig. 3c, where the action S is small. Here the approximate expression q(E) for the cross-section is a monotonically-declining function of the velocity that contains information only on the region of the potential U(R) that corresponds to distances $R \sim b_S$ (an optical analog of this is diffraction from an opaque screen).

However, when attraction and repulsion occur, the small-angle scattering corresponds also to a region of finite impact parameters (region II in Fig. 3c) near $b = b_g$, for which $\theta(b_g) = 0$, in addition to the region $b \sim b_S$. Hence, the way to make the cross-section more exact consists in taking account of the interference of the wave diffracted into the shadow region with the wave scattered at a small angle with $b \sim b_g$, and which corresponds to diffraction from a circular slit of radius b_g. Mathematically, this means that we must take account in the integral of (26) over the inner region $b < b_S$ of the contribution from the point b_g. The latter is the stationary-phase point of the function $\exp[2i\delta(b)]$ where the phase $\delta(b)$ passes through a maximum (see Fig. 1d). Thus, we derive the following cross-section q(E), which describes the so-called halo effect:

$$\left.\begin{aligned} q(E) &= \bar{q}(E) + \Delta q, \\ \bar{q} &= 2\pi b_z^2, \end{aligned}\right\}$$
$$\Delta q \approx 4\pi^{3/2} b_g \left(\frac{d^2\delta}{db^2}\Big|_{b=b_g}\right)^{-1/2} \cos\left[2\delta_g(E) - \frac{\pi}{4}\right], \qquad (27)$$

Here $\delta_g(E) = \delta(b_g, E)$ is the maximum phase of the scattering, and Δq is assumed to be small in comparison with $\bar{q}$. When E varies monotonically, the correction Δq proves to be an oscillating function of the energy.

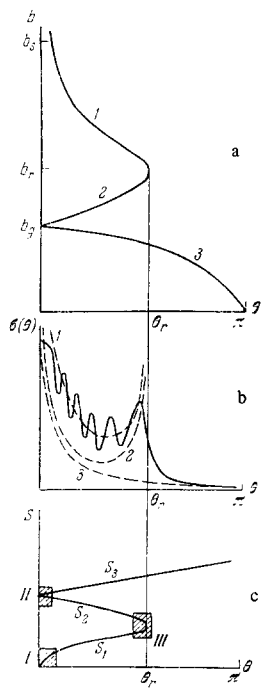

FIG. 3. Scattering functions, cross-sections, and quasiclassical actions for a potential having a minimum. a) The different branches $b_k(\theta)$ (k = 1, 2, 3) of the scattering function obtained by inversion of the function $\theta = \theta(b)$ given in Fig. 1b; b) the dotted curves (1, 2, 3) are the contributions from the different branches to the classical differential cross-section; the solid curve is the quantum cross-section; c) the quasiclassical section as a function of the scattering angle. The cross-hatched areas indicate the regions in which the quasiclassical description fails. The scattering in the region I is equivalent to diffraction from the edge of a screen, and that in region II is equivalent to diffraction from a circular slit.

A detailed review on the halo effect in atomic collisions is given in[28,29]. Figure 4, which is taken from[30], shows the oscillations in the total cross-section for scattering of Cs atoms by Hg. Analysis and interpretation of the oscillations become especially simple in the high-energy approximation (see below), in which the maximum phase proves to be inversely proportional to the velocity. That is, $\delta_g = \eta/v$. Hence we find on the basis of (27) that

$$\frac{\Delta q}{\bar{q}} \approx -\cos\left[\frac{2\eta}{v} - \frac{\pi}{4}\right] = -\cos[\pi(2N(E) + 1)], \qquad (28)$$

Here the experimentally-determined function N(E) takes on integral values at the maxima of Δq, and half-integral values at the minima of Δq. Figure 5 illustrates the relation of N to 1/v for the Cs-Hg system for which the total cross-section is shown in Fig. 4. In full agreement with (28), N proves to be a linear function of 1/v having the ordinate 3/8 at the origin. Measurement of the total cross-section makes it possible to determine the parameters of the long-range part of the potential (from the absolute value of $\bar{q}$ and the dependence of $\bar{q}$ on E), the "volume" of the potential well (from the frequency of oscillation of Δq), and a lower bound of the number of bound states in this well (from the number of extrema of Δq).[29]

The differential scattering cross-sections contain even more information on the potential.

Hoyt[31] first pointed out that one can reconstruct the potential U(R) from the classical differential cross-section. However, this method[31] required a knowledge of the cross-section $\sigma(\theta, E)$ at different energies E. Firsov[32] first showed that one can obtain

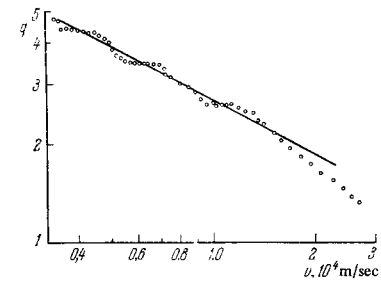

FIG. 4. Velocity-dependence of the total cross-section for scattering of Cs by Hg. The cross-section is in relative units. [30]

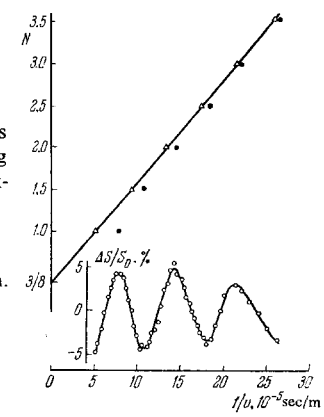

FIG. 5. Analysis of the oscillations of the total cross-section for scattering of Cs by Hg in the high-energy approximation. Circles: experimental results without account of the finite angular resolution. Triangles: the result of taking account of the finite resolution. [30]

the potential function from differential cross-section data at a fixed energy. Ideally, with absolutely accurate measurements, it suffices to know the cross-section $\sigma(\theta, E)$ at all angles $0 < \theta < \pi$ for a single value of the energy E. Actually, however, we know the cross-section (and with limited accuracy) only in a limited region, most often at small angles. This is because of the sharp decline in the intensity of the scattered flux with increasing angle. In such a situation, it is convenient to treat the experimental data directly in an approximation that corresponds to scattering for large energies at small and medium angles. In this case, the solution of the inverse problem takes on an especially simple form.[32]

In this regard, let us turn to the limit of high energies. We shall treat a transition from the overall quasiclassical description given by Eqs. (20)—(25) to the high-energy "impact parameter" approximation presented in Chap. 2. To do this, it suffices to retain the larger term in the expansion of the scattering functions (22), (24), and (25) in terms of the parameter U(R)/E (a systematic expansion has been carried out in[33,34]). Here the radial action (19) equals

$$2\delta(b, E) = \frac{2}{v}\int_b^\infty \frac{U(R)\,dR}{\sqrt{1-b^2/R^2}} + O(U/E) \qquad (29)$$

It proves to coincide with the phase (18) of the amplitude A(b) in the impact-parameter method. It will be convenient henceforth to transform to new variables, the reduced angle τ and the reduced cross-section ρ, according to the formulas

$$\tau = E\theta, \qquad (30)$$

$$\rho(\tau, E) = \theta \sin\theta\sigma(\theta, E). \qquad (31)$$

In terms of the new variables, the action (22) can be written to an accuracy of the terms O(U/E), which will be omitted henceforth, in the form

$$S^{\pm}(b, E, 0) = \frac{1}{v} s_0^{\pm}(b, \tau), \qquad (32)$$

Here the reduced action $s_0^{\pm}(b, \tau)$ equals

$$s_0^{\pm}(b, \tau) = -2\int_b^\infty \frac{U(R)\,dR}{\sqrt{1-b^2/R^2}} \pm 2b\tau \pm i\frac{\tau}{\lambda}. \qquad (33)$$

Equation (24), which defines the classical scattering angle as a function of the impact parameter, will have the form

$$\tau(b) = \pm b\int_b^\infty \frac{1}{R}\frac{dU}{dR}\frac{dR}{\sqrt{1-(b^2/R^2)}}, \qquad (34)$$

It exactly coincides with the classical formula (9) for scattering at small angles. By inverting (34), we find that the impact parameter b is a function of τ alone, apart from higher terms in U/E:

$$b = b(\tau). \qquad (35)$$

Since $1/E = \theta/\tau$, an expansion in terms of 1/E at fixed angle can be treated in the same way as an expansion in the small angle at fixed energy.

One can easily show from the ordinary expression (3) for the cross-section that the corresponding reduced cross-section has the form

$$\rho(\tau, E) = \frac{1}{2}\frac{d(b^2)}{d\ln\tau} = \rho_0(\tau) + O(1/E). \qquad (36)$$

This equation expresses a very important principle of correspondence that was first formulated in[33]. It states that the reduced cross-section becomes a function of only one variable $\tau = E\theta$ in the limit of small angles or large energies.

This means that experimental data obtained at different energies (from thermal energies to 500 keV) can be fitted in terms of the reduced parameters ρ and τ to a single curve $\rho_0(\tau)$, or to a family of curves having a common envelope $\rho_0(\tau)$. This substantially increases the accuracy and reliability of the experimental $\rho_0(\tau)$ curve, which we can use in turn in a simple way to solve the inverse problem.

In fact, if we have data over a broad enough region of τ, then by integrating (36), we find

$$b_0^2(\tau) = \int_\tau^\infty \rho_0(\tau')\,d\ln\tau'. \qquad (37)$$

However, the function $\tau_0(b)$ that is the inverse of (37) is directly related to the scattering potential U(R) according to Eq. (34). from which we get directly

$$U(R) = \frac{2}{\pi}\int_R^\infty \frac{\tau_0(b)\,db}{(b^2-R^2)^{1/2}}. \qquad (38)$$

Equation (38) is a special case of the formula of Firsov,[29] which corresponds to high energies. Thus, the procedure of obtaining the potential U(R) from data on scattering at large energies reduces to (37) and (38), and proves to be relatively simple.

As an example, we shall take up an analysis of elastic-scattering data in the He^+—Ne system.[35] Figure 6 gives the reduced cross-sections for elastic scattering (and quasielastic scattering at high energies) of He^+ by Ne, as obtained by different authors at different energies and angles. The parameters of the potential have been reconstructed[35] from these data; it is described by a combination of Coulombic repulsion, which is shielded by the electron cloud of Ne, combined with polarization attraction at large distances. We note another characteristic feature of the elastic-scattering curves, which can be ascribed to

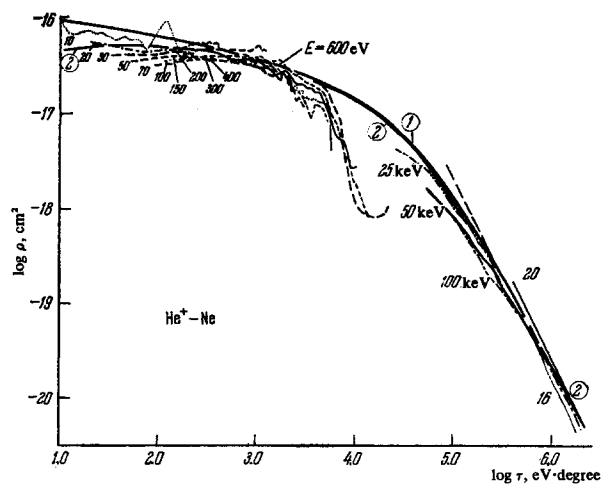

FIG. 6. Cross-sections for elastic and quasielastic scattering of He^+ by Ne in terms of the reduced variables ρ and τ for different energies. [35] 1 and 2 are the theoretical curves for different approximations of the scattering potential.

interaction between electronic states. This is the oscillating structure superposed on the smooth variation of the cross-section. For any value of the energy, it begins at a quite definite value of the reduced angle $\tau = 1950$ eV-degree. Hence, it is due to a process that occurs at a quite definite internuclear distance $b_c = b(\tau_{thr}) \simeq 1.9\ a_0$. It was shown in[35,36] that these anomalies arise from the quasi-crossing at the point $R \approx b_c$ of the ground and excited terms, and that the point $\tau = \tau_{thr}$ corresponds to the threshold of the inelastic channel. We shall return in Chap. 5 to a more detailed discussion of this phenomenon in treating inelastic processes. One can find other examples of reconstruction of a potential from elastic-scattering data, e.g., in[9,37,38].

The advantages and simplicity of the reduced impact-parameter approximation are also manifested in an analysis of the fine interference structure of scattering cross-sections at large energies. In fact, the phase of the oscillations of the cross-section in (25) is determined by the action difference ΔS between different trajectories. For oscillations of the total cross-section in (27), it is determined by the action at $\theta = 0$. However, at large energies, the relation of the action to the energy at fixed τ is determined by the coefficient $1/v = \mu/\sqrt{2\mu E}$, according to (32) and (33). Hence, the phase of the oscillations is a linear function of the reciprocal of the velocity. That is, the period of oscillation of the cross-section as a function of $1/v$ is a constant. The high-energy approximation also makes it possible to derive relatively simple expressions for the scattering cross-section at small angles. The approximation of an opaque screen containing a slit, while satisfactory for calculating the total cross-section according to (27), proves to be unsuitable generally for calculating the differential scattering at angles $\theta \approx \pi/b_S$: the diffuseness of the potential is important in this region, but not substantial in the region of the first diffraction maximum for $\theta < \pi/b_S$. More detailed treatment shows[7] that the oscillating structure of the cross-section at $\theta \sim \pi/b_S$, which might be expected by analogy with diffraction by a screen, is completely blurred out by the diffuseness of the potential. Thus the first peak of the diffraction maximum with increasing θ smoothly goes over into the $\sigma(\theta)$ function that describes classical scattering at small angles. Experimental study of this region makes it possible to determine the parameters of the long-range portion of the potential. Figure 7 gives one of the few examples of studying scattering in the small-angle region, including the classical and quantum regions.

We shall now take up interference phenomena in large-angle scattering. We see from Fig. 3 that interference occurs between three branches of the function $b_i = b_i(\theta)$ when $\theta < \theta_r$. However, one can resolve experimentally only the low-frequency oscillations due to interference of waves from branches 1 and 2.* This interference is analogous to that which occurs in rainbow formation, and the corresponding theory is a special case of the theory of scattering of waves at an extremal angle.

*High-frequency oscillations (interference from three branches of the $b(\theta)$ function) have recently been detected experimentally in the differential cross-sections for scattering of inert-gas atoms. [108]

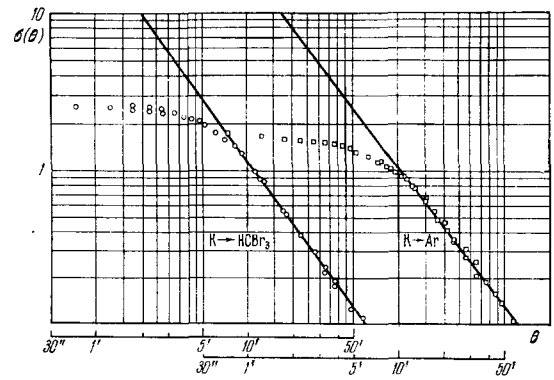

FIG. 7. Scattering cross-sections (in relative units) of K by Ar and by $HCBr_3$ at small angles.

When $\theta < \theta_r$ (the bright side of the rainbow), the classical differential cross-section of (3) increases monotonically as $\theta \to \theta_r$, and it diverges like $(\theta_r - \theta)^{1/2}$ near θ_r. The quasiclassical description (25) gives oscillations on the bright side of the rainbow. However, it does not permit us to follow the transition through the angle θ_r, since the stationary-phase method is inapplicable in this case.[20,24] A parabolic approximation of the function $\theta = \theta(b)$ near b_r, with account taken of the merger of the two stationary-phase points (the region 1—2, Fig. 3b) gives the following expression for $\sigma(\theta)$ near θ_r in terms of an Airy function:[27]

$$\sigma(\theta) = \frac{2\pi b_r}{\sin\theta}\,|y|^{-2/3}\,\Phi^2(|y|^{-1/3}(\theta-\theta_r)),\quad y = 2\pi^2\frac{d^2\theta}{db^2}\Big|_{b=b_r}. \qquad (39)$$

This formula describes the exponential decay of intensity on the dark side of the rainbow and the first several oscillations on the bright side as well. Then the quasiclassical asymptotic behavior of the Airy function makes it possible to join (39) with the general formula (25). The transition of rainbow oscillations into oscillations at small, but classical angles that correspond to the halo effect has been discussed in[39].

Experimental study of scattering in the rainbow region permits one to get information on the depth of the potential well (from the size of the angle θ_r) and on the interatomic distance R_m that corresponds to the potential minimum (from the frequency of oscillation of $\sigma(\theta)$ on the bright side of the rainbow).[40] Figure 8 illustrates the possibilities of experimentation on resolution of rainbow structure.[41]

Finally we note another reason for oscillations of the differential cross-section in scattering of identical

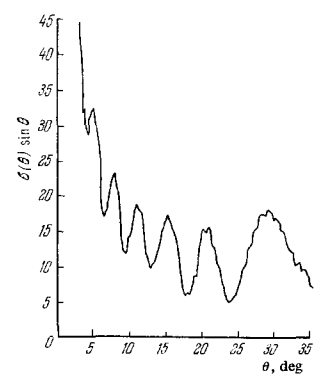

FIG. 8. Rainbow scattering of Na by Hg. [41] The cross-section is in relative units.

atoms, as predicted by Mott.[42] Since the waves corresponding to the impinging particle and the target can interfere, the observed cross-section (which is evidently symmetrical with respect to the angle $\theta = \pi/2$) is

$$\sigma(\theta) = |f(\theta) \pm f(\pi - \theta)|^2,$$

Here the sign ± depends on the type of statistics of the nuclei. Figure 9 shows the scattering cross-section of ^{20}Ne by ^{20}Ne for the energy $E \approx 10^{-13}$ ergs (circles).[43] The solid line shows the result of calculating $\sigma(\theta)$ for a Lennard-Jones potential, while the dotted line is the scattering cross-section without account taken of identity, for which $\sigma(\theta) = |f(\theta)|^2$.

4. INTERFERENCE IN RESONANCE PROCESSES

Experimental study of scattering when several channels exist (inelastic scattering) gives specimens of a very rich interference pattern of the cross-sections that is much more complex than in ordinary potential scattering. A special place among inelastic processes is occupied by resonance symmetrical processes, such as spin exchange, excitation transfer, and charge transfer. This involves the fact that the result of collision can be described in terms of interference of waves scattered by different potentials, and corresponding to different (even and odd) electronic molecular states, without any transitions between these states. In this sense, the two-level problem of a symmetrical process is a very simple generalization of the one-level problem, and all the results of the last chapter can be used directly to construct an appropriate theory.

Charge transfer is apparently the most fully studied of all the symmetrical processes. It has been studied in the following atomic systems: H^+—H,[44,45] He^+—He,[46-49] Li^+—Li,[50] Ne^+—Ne.[51] Hence, for the sake of concreteness, we shall treat this type of processes in particular.

In the very simple case of charge transfer of an s electron, one should describe the physically observable situation, in which the charge is localized on one of the particles before and after scattering, by a linear combination of an even g and an odd u state. Here the probability P(b) of charge transfer for a straight-line trajectory with an impact parameter b is determined by the difference of phases in (19) incurred as a result of collision in potentials U_g and U_u, respectively:

$$P(b, E) = \sin^2\left[\frac{1}{\hbar v}\int_b^\infty (U_g - U_u)\frac{R\,dR}{\sqrt{R^2 - b^2}}\right] = \sin^2[\Delta\delta(b, E)]. \quad (40)$$

This expression, which corresponds to the high-energy approximation, predicts (in full analogy with the halo effect in elastic scattering) that the total charge-transfer cross-section will be oscillatory in nature if the phase difference of elastic scattering in the even and odd states passes through an extremum.[52,53] A calculation of the total charge-transfer cross-section $q_{c.t.}$, with account taken of the region of slow probability oscillations, gives

$$q_- = 2\pi\int_0^\infty b\,dbP(b, E) = \bar{q}_- + \Delta q_-,$$

Here $\bar{q}$ is the monotonic component of the cross-section, while Δq is the oscillating additive term:

$$\bar{q}_- = \frac{\pi}{2}b_s^2,$$
$$\Delta q_- = -\pi^{3/2}b_m\left(\frac{d^2\Delta\delta}{db^2}\Big|_{b=b_m}\right)^{-1/2} \times \cos[2\Delta\delta - \pi/4]. \quad (41)$$

The impact parameters b_s and b_m are determined by the conditions

$$\Delta\delta(b_s) \approx 1,$$
$$\frac{d\Delta\delta}{db}\Big|_{b=b_m} = 0,$$

We can make the first condition more precise by performing the stated integration over b with account taken of the correct asymptotic form of $U_g - U_u$, instead of using the random-phase approximation near the charge-transfer boundary.[54,5] Figure 10 shows the energy-dependence of the total charge-transfer of some alkali-metals.[55] This dependence has been used in[64] to determine the parameters of the proposed analytical expression for $\Delta U(R)$.

The formula (40) for the charge-transfer probability permits one to give a qualitatively correct description[48] even of the oscillations of the differential cross-section for scattering with charge transfer. To do this, we make θ (the scattering angle in the mean potential $\bar{U} = \frac{1}{2}(U_g + U_u)$) correspond to the impact parameter according to Eq. (9). Figure 11 (from[48]) shows a diagram of the maxima of the charge-transfer probability $P(\theta, E)$ for He^+—He, as obtained experimentally and as calculated by Eq. (40). It was shown in the same study[48] that, as we should expect from (40), the experimental phases of the oscillations $2\pi N(\tau, E)$ for fixed values of the reduced angle $\tau = \theta E$ prove[47,48] to

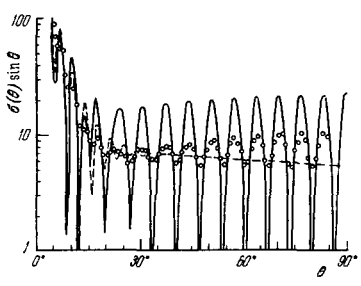

FIG. 9. Oscillatory structure of the scattering cross-section of Ne^+ by Ne arising from identity of the atoms. [43]

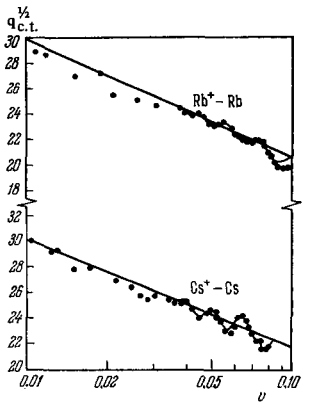

FIG. 10. Velocity-dependence of the cross-section for resonance charge transfer $q_{c.t.}$ of Rb and Cs atoms. [55] The straight lines describe the monotonic component of $q_{c.t.}$. The cross-sections and the velocity are in atomic units.

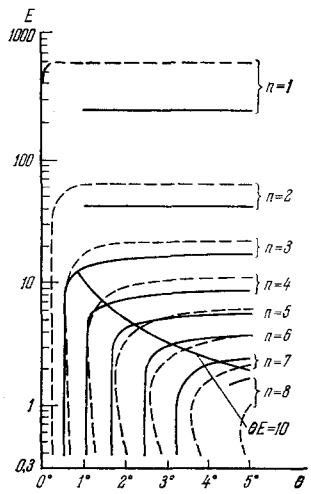

FIG. 11. Diagram of the probability maxima for charge transfer of He^+ with He as a function of the scattering angle and the energy. [48] Solid lines: experimental data; dotted lines; theoretical calculations.

be linear functions of 1/v. (However, they do not vanish as $1/v \to 0$ as Eq. (40) would require.) Here the slopes of the lines for large enough τ ($b \to 0$) do not depend on τ, and they give the value of the integral at b = 0

$$I(0) = 2\int_0^\infty [U_g - U_u]\, dR. \tag{42}$$

For example, the experimental value I(0) = 63.7 eV-Å for charge transfer of H^+ with H[45] proves to be close to the value 70.2 eV-Å calculated from the potentials of H_2^+ known from[57]. The situation has been somewhat more complicated in interpreting the oscillation period in the He^+—He system. In order to explain the observed value of I(0), Lichten[16] suggested that motion in the $^2\Sigma_g$ state does not follow the lower adiabatic term, for which an independent estimate of I(0) has given a much lower estimate. Rather it follows the adiabatic $^2\Sigma_g$ term, which in the one-electron approximation corresponds to the configuration $(1\sigma_g)(1\sigma_u)^2$ of the He_2^+ system. Figure 12 (from[16]) shows the terms of this system. When $R < 2a_0$, the diabatic term $1\sigma_g 1\sigma_u^2$ crosses the terms of the same symmetry, and when $R < 1.3\ a_0$, the state becomes autoionizing. However, the excellent agreement of the observed interference pattern with Lichten's predictions[16] shows that we can neglect the interaction that gives rise to

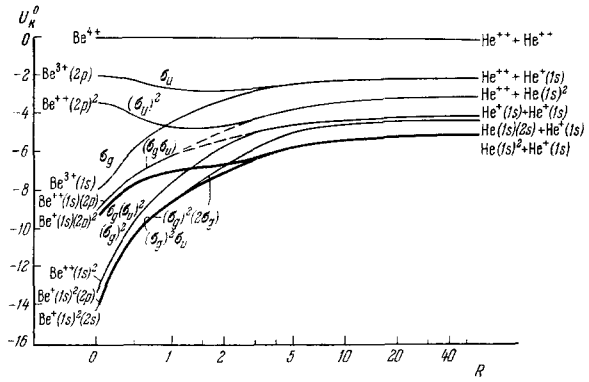

FIG. 12. Correlation diagram of the terms in the He_2 system during transition to the united ion Be^+. [16] Energies and distances in atomic units.

transitions at the crossings of the Σ_g terms at high velocities, and the motion actually occurs along the stated diabatic term.

However, this description could not explain a number of observed phenomena, first of all, the damping of the oscillations, i.e., the fact that the experimental oscillations in the cross-section do not go to zero. Hence, a stricter quasiclassical description was proposed in[58,59] that is valid also at small energies.

The quantum cross-sections with or without charge transfer are[60]

$$\sigma_\pm(\theta, E) = |f_g(\theta, E) \pm f_u(\theta, E)|^2, \tag{43}$$

where $f_{g,u}$ are the scattering amplitudes in the potentials $U_{g,u}$, respectively. If we use the quasiclassical expressions for the amplitudes, we get the cross-sections $\sigma_\pm$ in the following form (we assume for simplicity that there is no rainbow scattering from the lower term at the given θ and E):

$$\sigma_\pm(\theta, E) = |\sigma_g^{1/2}(\theta, E)\, e^{iS_g(b_g, \theta, E) + i\gamma_g} \pm \sigma_u^{1/2}(\theta, E)\, e^{iS_u(b_u, \theta, E) + i\gamma_u}|^2. \tag{44}$$

Here the action S and the impact parameter b are related to the potential at a given E and θ by Eqs. (22) and (23), and σ_g and σ_u are the elastic-scattering cross-sections in the fields U_g and U_u.

Thus, trajectories corresponding to different impact parameters b_g and b_u from each of the two terms contribute to interference at the given angle θ. Since σ_g and σ_u differ, the cross-section of (44), which oscillates between the envelopes $|\sigma_g^{1/2} \pm \sigma_u^{1/2}|^2$, has a finite (non-zero) value at the minima, in contrast to the results of Eq. (40). The maxima and minima of the oscillations in the cross-section are approximately the extrema of the function

$$\cos(S_g - S_u + \Delta\gamma) = \cos 2\pi N(E, \theta), \tag{45}$$

Here $N(E, \theta)$ is the previously-discussed experimental function that takes on integer values at the maxima, and half-integer values at the minima of the cross-section. The derivative of this function with respect to θ at a fixed energy is related to the period $\Delta\theta$ of the oscillations with respect to angle,

$$1/\Delta\theta = \left(\frac{\partial N}{\partial \theta}\right)_E, \tag{46}$$

In view of the relation $b = \pi\partial s/\partial\theta$, it can be used to get an important characteristic, namely, the difference $\Delta b = b_g - b_u$ between the two impact parameters that contribute to interference:

$$\Delta b = \frac{2\pi\hbar}{v}\frac{\partial N}{\partial\theta} = \frac{mv}{2}\frac{d\Delta S}{d\tau}. \tag{47}$$

Since $S \sim s(\tau)/v$, then, at large energies, the quantity in (47) depends only on one variable τ, or on the impact parameter, and it does not depend on the energy at fixed τ.

The stated quasiclassical description substantially improves the agreement with experiment, especially at low energies.[61,62] Figure 13, which is taken from[63], compares the theoretical and experimental curves of the differential cross-section as a function of the scattering angle for He^+—He at 300 eV. It demonstrates the effects of the nuclear symmetry, which are analogous to those described in Chap. 2 for Ne_2 (see Fig. 9), and which lead to additional oscillations in the system

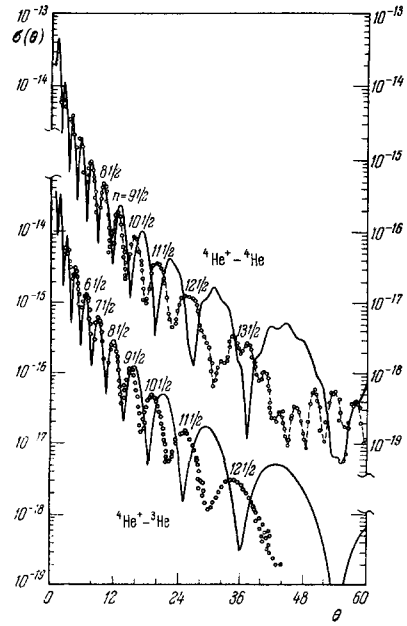

FIG. 13. Differential cross-sections for charge transfer of $^4He^+$ with ^4He and $^3He^+$ with ^4He. [63]

of identical nuclei $^4He^+-^4He$, as compared with the system $^4He^+-^3He$.

However, an interpretation of experiments on symmetrical resonance charge transfer in the two-state approximation does not permit one to explain a certain effect: the small systematic variation in the phase of the oscillations. According to (40) or (45), the two-level approximation predicts that the phase should be proportional to the reciprocal of the velocity. Hence, the phase should approach zero as $1/v \to 0$. Nevertheless, extrapolation of the phase to $1/v \to 0$ gives a finite value in experiments both for H^+-H,[44] and for He^+-He.[47,48] Detailed study of this problem for the H^+-H charge transfer shows[64] that Coriolis interaction of the electron with the rotating molecular axis becomes very substantial at large velocities and small impact parameters. One must get outside the framework of the two-level approximation to describe this effect. This interaction is especially effective for those molecular states of different symmetries that correlate with the same atomic state in the united-atom limit, which is just what happens in the H_2^+ system. One of the terms participating in charge transfer (namely, the term $^2\Sigma_u$ and the term $^2\Pi_u$), which corresponds as $R \to \infty$ to excitation of an H atom, proves to be degenerate in the limit $R \to 0$. This is because the corresponding states in this limit are two components ($p\sigma$ and $p\pi$) of the 2P state of the united atom (He^+). A general theory of such a $\Sigma-\Pi$ non-adiabatic coupling is given in[65,66]. This coupling both makes possible inelastic transitions (and hence it is also the reason for damping of the oscillations), and it shifts the phase of the oscillations in the elastic channel. Scattering calculations in the H^+-H system[67,68] with account taken of the large number of states give a theoretical curve fully agreeing with the data of Everhart (see[45]), both in amplitude and in phase of the oscillations (Fig. 14). While the data[45] contained no information on the excited states of the products,

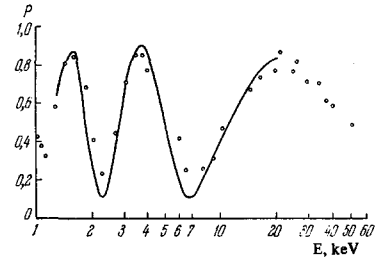

FIG. 14. Comparison of the theoretical [68] (solid line) and experimental [45] (points) probabilities for charge transfer of H^+ with H.

nevertheless the phase of the oscillations proved to be so sensitive that it permitted a prediction of an appreciable probability of inelastic scattering in the 2S state. This prediction has been recently confirmed experimentally[69] by measuring the differential cross-section for scattering of excited atoms in collisions of H with H^+.

5. SPECTROSCOPY OF INELASTIC PROCESSES

In contrast to resonance processes, such as the above-discussed charge transfer, the total cross-sections of inelastic processes as functions of the velocity show a characteristic broad maximum at some velocity v_m. From a description of such a behavior of the total cross-sections, it has been possible to reveal an important parameter on which the cross-sections of inelastic processes depend: the adiabaticity or Massey parameter $\xi = \omega\tau$. It is equal to the product of the characteristic frequency ω of the transition by the characteristic time τ of the transition. An inelastic process occurs with an appreciable probability only when $\xi \leq 1$. If we write this criterion in the form

$$\xi = \frac{\Delta E}{\hbar}\frac{a}{v} \leqslant 1, \qquad (48)$$

where ΔE is the energy of the inelastic transition and a is the characteristic atomic dimension, then we can easily convince ourselves that most inelastic processes should occur with an appreciable probability only in the kilo-electron-volt range of energies. Nevertheless, numerous experiments show that excitation processes, as a rule, have large cross-sections at much lower energies than are predicted by the simple criterion of (48). These energies sometimes nearly approach the energy threshold of the process in question. As an example we shall point out that ionization can occur at an energy below 100 eV, even in such a system as Na^+, Ne,[70] where the atomic shells resemble those of an inert gas.

The reason for such a seeming contradiction consists in the fact that the actual transitions occur in regions of approach or quasi-crossing of the terms. Therefore, the crude criterion of (48) should be replaced by a more refined criterion involving the Massey parameter as determined by Eq. (6). If here the energy gaps to the other terms are large enough (the corresponding Massey parameters are large), then the inelastic process can be described on a basis of two electronic states.

Upon limiting ourselves to the two-state approxima-

tion, we shall assume that the adiabatic functions $\varphi_i(\mathbf{r}, \mathbf{R})$ are given. Then, by a linear transformation, we can unambiguously construct two functions $\varphi_i^0(\mathbf{r})$ of the diabatic basis from the condition $\langle \varphi_1^0 | \partial/\partial R | \varphi_2^0 \rangle = 0$, with the supplementary condition that $\varphi_i^0(\mathbf{r}) = \lim_{R\to\infty} \varphi_i(\mathbf{r}, \mathbf{R})$. The overall wave function of the colliding atoms can be represented in the form of an expansion*

$$\Psi(\mathbf{r}, \mathbf{R}) = \sum_{l,m} \frac{1}{R} Y_{lm}\left(\frac{\mathbf{R}}{R}\right)[\varphi_1^0(\mathbf{r})\chi'_{1,l}(R) + \varphi_2^0(\mathbf{r})\chi^0_{2,l}(R)]. \quad (49)$$

The total cross-section and amplitude of the differential scattering cross-section in either given state n(n = 1, 2) for the initial state n_0 are expressed by summations over the angular momenta l. As usual the latter can be replaced by integrals over the impact parameters

$$\sigma_{nn_0}(E) = 2\pi \int_0^\infty b\, db P_{nn_0}(b), \quad P_{nn_0} = |S_{nn_0} - \delta_{nn_0}|^2, \quad (50)$$

$$f_{nn_0}(\theta, E) = -\frac{2\pi k_0}{\sqrt{\sin\theta k}} \int_0^\infty \sqrt{b}\, db S_{nn_0}(b)\left[e^{ikb\theta - i\frac{\pi}{4}} + e^{-ikb\theta + i\frac{\pi}{4}}\right], \quad (51)$$

Here $S_{nn_0}(b)$ is the transition matrix, whose elements for a given partial wave are determined by the asymptotic behavior of the radial wave functions $\chi'_{n,l}$ at large distances:

$$\chi'_{n,l}(R) \sim \frac{1}{\sqrt{k}}[\delta_{nn_0}e^{-ikR} + S_{nn_0}e^{ikR + i\pi l}]. \quad (52)$$

At finite R, these functions obey the Schrödinger equation

$$\frac{1}{2\mu}\frac{d^2}{dR^2}\chi'_{n,l}(R) + \sum_{m=1,2}\left[\left(E - \frac{\hbar^2 l(l+1)}{2\mu R^2}\right)\delta_{nm} + U_{nm}(R)\right]\chi'_{m,l}(R) = 0. \quad (53)$$

One can show (see, e.g.[71]) that at high energies and large values of l that satisfy the condition

$$E \gg U_{nm}(b), \quad b = \lambda l,$$

the amplitudes S_{nn_0} determined by Eqs. (52) and (53) coincide with the amplitudes A_{nn_0} found by solving the first-order high-energy equations (13). This limiting case corresponds to small-angle scattering.

Thus, in contrast to elastic scattering, one must solve the equations (53) to find the amplitudes of the transitions, or the equations (13) in the special case of high energies. These solutions depend substantially on the nature of the terms that characterize the given two states. In many cases, inelastic processes can successfully be described in terms of a quasi-crossing model or the so-called Landau-Zener model and its generalizations.

*The form of this representation assumes that the angular momentum with respect to the motion of the atoms is conserved. Together with limiting the coupling between the two states, this means that the expansion in (49) is applicable, strictly speaking, to describing inelastic processes that involve only s electrons. However, the two-level approximation can actually be applied successfully also to processes that change the orbital angular momentum of the electron. To do this, one must consider individual regions of non-adiabaticity, and construct the total scattering matrix by merging the solutions inside and outside these regions.

Figure 15 shows a typical pattern of terms that illustrates the model. In the vicinity of the quasi-crossing, the terms of the system $U^0_{11}(R)$, $U^0_{22}(R)$ that are calculated in a certain "zero-order" approximation (i.e., upon neglecting some interaction) intersect at the point R_p. We shall consider the zero-order approximation basis that corresponds to them to coincide with the diabatic $\varphi'_k(\mathbf{r})$. Taking account of the interactions that are omitted in the "zero-order" approximation, which we can consider to be constant in a small neighborhood of R_p, leads us to a model Hamiltonian on the diabatic basis:

$$U^0_{nm}(R) + \frac{\hbar^2 l(l+1)}{2\mu R^2} = U_p + \frac{\hbar^2 l(l+1)}{2\mu R_p^2} + \begin{pmatrix} -F_1(R-R_p) & V_{12} \\ V_{21} & -F_2(R-R_p) \end{pmatrix}, \quad (54)$$

It is valid in the small neighborhood of the quasi-crossing. Here the slopes of the terms F_n include the centrifugal force and $U_p = U^0_{11}(R_p) = U^0_{22}(R_p)$. The adiabatic potentials

$$U_{1,2}(R) = U_p - \frac{F_1+F_2}{2}(R-R_p) \pm \left[\frac{\Delta F^2}{4}(R-R_p)^2 + V_{12}^2\right]^{1/2} \quad (55)$$

naturally obey the rule of no crossing of terms of like symmetry.

A solution of the system of equations (53) or (13) with the potential matrix of (54) has been derived by Landau,[72] Zener,[73] and Stueckelberg[23] for the case in which the energy E_R of radial motion in the crossover region is substantially greater than the minimum splitting of terms:

$$E_R = E - U_p - \frac{\hbar^2 l(l+1)}{2\mu R_p^2}, \quad (56)$$

and it varies little throughout the transition region $\Delta R \approx (2V_{12}/\Delta F)$:

$$E_R \gg \Delta R \frac{dU^0_k}{dR}. \quad (57)$$

These conditions are equivalent to the possibility of introduction in the transition region of a single trajectory for both terms $R(t) = R_p - v_R(t - t_0)$ having the constant velocity $v_R = \sqrt{2E_R/\mu}$. With the Hamiltonian of (54), this gives a model that can be achieved exactly. By studying this model, the probability

$$P = e^{-\pi\delta} \quad (58)$$

of transition from one adiabatic term to the other during a single passage through the non-adiabatic region has been found.[72,73,23] The parameter

$$\delta = \frac{2V_{12}^2}{\hbar v_R \Delta F} \quad (59)$$

is the Massey parameter of the given model ($\omega \approx 2V_{12}/\hbar$, $\tau \approx \Delta R/v_R = V_{12}/\Delta F v_R$). We see from

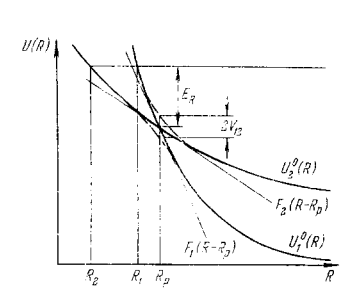

FIG. 15. Parameters of the Landau-Zener model.

(58) that the motion mainly follows the adiabatic terms at low velocity ($\delta \gg 1$), but the diabatic terms at high velocity ($\delta \ll 1$).

The total transition probability (with two passages through the point R_p) is

$$\mathcal{P}_{12}(b, E) = 2P(1-P)(1-\cos\varphi). \quad (60)$$

The phase φ of the probability oscillations is approximately equal to the difference between the quasiclassical actions for the two transition paths upon double passage through the quasi-crossing region:

$$\varphi = 2\int_{R_1}^{R_p} k_1\,dR - 2\int_{R_2}^{R_p} k_2\,dR + \gamma_I - \gamma_{II}, \quad k_i = \frac{\sqrt{2\mu}}{\hbar}\left[E\left(1-\frac{b^2}{R^2}\right) - U_i^0\right]^{1/2} \quad (61)$$

Figure 15 explains the meaning of the points R_i. The angular displacements γ_I and γ_{II} are additional phase changes in the transition region. They were studied in[74,75], where they also found the total matrix A_{nn_0} of the transitions. The possibility that is reflected in (60) of treating independently the transitions as the atoms approach and as they fly apart requires the condition that the value of the phase φ should be large:

$$\varphi \gg 2\pi. \quad (62)$$

In calculating the total inelastic cross-section of (50) in the expression (60) for the transition probability, we must average over the large phase φ. Consequently, the relation of the inelastic cross-section to the energy of the atoms shows a characteristic maximum at a velocity $v \sim 2.34 \cdot 2\pi V_{12}^2/\Delta F$.[5] This behavior is characteristic of many cross-sections for non-resonance charge transfer, excitation, etc.

However, even within the framework of the same system of intersecting terms, the Landau-Zener formula (60) proves to be inapplicable at small energies ($E < U_p$), or at large impact parameters ($b \gtrsim R_p$). In fact, the crossover point then proves to be close to the turning points in the radial motion. This involves violation of the conditions (56) and (57) for uniformity and classical nature of motion in the transition region as well as the condition (62) for independence of the transitions during forward and reverse passage through the transition region. Hence, the total inelastic cross-section of a process having a high energy threshold, i.e., having a large value of the potential U_p at the crossing point, begins to deviate from that predicted by the Landau-Zener theory at energies E close to U_p. Apparently, such a deviation has been found in[74] for excitation processes in the Cs^+—He system, and it is shown in Fig. 16.* In just the same way, the Landau-Zener theory is inapplicable also for describing differential scattering cross-sections at angles close to threshold scattering angles.

All that we have said indicates that the theory must be extended to the case of small energies E_R in the transition region, in which the crossing point is close

*It was emphasized in [75] that there can be another reason for deviation of the observed relations from those predicted by the Landau-Zener theory, in addition to the effect of closeness of the turning point to the crossing point. This is the existence of several (more than two) channels for the process, if the thresholds of these processes are close together.

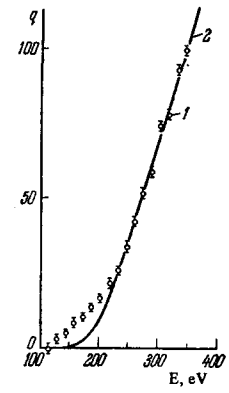

FIG. 16. Threshold behavior of the total cross-section for excitation of Cs^+ in collisions with He. Points: experimental data; [83] solid line: calculated by the Landau-Zener formula with parameters that make the theory agree with experiment at high energies.

to the turning points of radial motion. Hence, we need a quantum description of the radial motion. We shall present briefly the results of such a study, which was performed in[76-80]. In[78], the quantum equations (55) were studied for the functions $\chi_n(R)$ for radial motion in the model (56) of linear terms for an arbitrary energy $E_R = E - U_p - [\hbar^2(l+1/2)^2/R_p^2]$ of radial motion at the crossing point. It turns out that when $F_1F_2 > 0$ (the slopes of the terms have the same sign), the problem of quantum transitions in the system of (56) is exactly equivalent to the problem[76] of transitions in the semiclassical formulation with a defined selection of a trajectory $R = R(t)$. Namely, the probabilities and amplitudes of transitions can be calculated for the system of equations

$$i\frac{d}{dt}\begin{pmatrix} c_1 \\ c_2 \end{pmatrix} = \begin{pmatrix} -F_1[R(t)-R_p] & V_{12} \\ V_{21} & -F_2[R(t)-R_p] \end{pmatrix}\begin{pmatrix} c_1 \\ c_2 \end{pmatrix}, \quad (63)$$

if we define the trajectory as being the trajectory of motion in a homogeneous potential field having the force $F = (F_1F_2)^{1/2}$, i.e.,

$$R(t) = R_p + \frac{F}{2\mu}t^2 + \frac{E_R}{F}. \quad (64)$$

One can easily show from (64) and (63) that the probability $\mathcal{P}(b)$ of the transition is a function of only two dimensionless parameters

$$\varepsilon = \frac{E_R\Delta F}{2V_{12}F}, \quad \eta = \frac{4V_{12}}{\hbar}\left(\frac{\mu V_{12}}{|\Delta F F|}\right)^{1/2} \quad (65)$$

and it can be studied analytically in the limiting cases of large ($\eta \gg 1$) and small ($\eta \ll 1$) splittings of the adiabatic terms for any energies E_R (or for any values of the dimensionless parameter ϵ). In the former case, in which $\eta \gg 1$, the transition probability is an exponentially small quantity (see also[79]):

$$\mathcal{P} = B(\varepsilon)e^{-\eta\Delta(\varepsilon)}. \quad (66)$$

Figure 17 shows the function $\Delta(\epsilon)$. A calculation of the inelastic cross-section[107] with account taken of the deviation of the probability in (66) from (60) explains the deviation depicted in Fig. 16 of the experimental

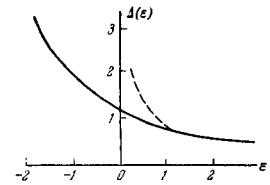

FIG. 17. Graph of the function $\Delta(\epsilon)$ that determines the value of the exponential factor of the transition probability in the adiabatic region ($\eta > 1$) (solid curve). Dotted curve: Landau-Zener approximation.

cross-section from that depicted by the Landau-Zener theory at energies near the threshold of the inelastic process in the Ca^+—He system.

When the splittings of the terms are arbitrary (η has any value), the same form (66) describes the exponentially small probability of a tunnel transition whenever $\epsilon < 0$. In this case, only the form of the coefficient $B(\epsilon)$ in front of the exponential is changed.

For small splittings of the terms ($\eta < 1$), the transition probability can be found by the perturbation theory from the interaction V_{12} between the diabatic states (see also[22], p. 390). It is determined by the formula

$$\mathcal{P} = \pi\eta^{4/3}\Phi^2(-\epsilon\eta^{2/3}), \tag{67}$$

where Φ is Airy's function. When the value of the argument is larger in modulus, Eq. (67) goes over into the Landau-Zener formula (60) for $\epsilon > 0$, and into (66) for a tunnel transition when $\epsilon < 0$.

It is of interest to furnish an experimental proof of this pattern of transitions that has been obtained by methods of molecular (not collisional) spectroscopy. Figure 18, which is taken from[81], shows the probability $\mathcal{P}(E)$ of predissociation, i.e., decomposition of an O_2 molecule under the influence of a non-adiabatic transition to the repulsive term $U_1(R)$ as a function of the vibrational energy E in the initial stable term $U_2(R)$ (the plotted points are taken from[82]). The solid curve is calculated by Eq. (67) with adjustment of three parameters (the scale in η, the scale in ϵ, and the reference origin E). The dotted curve shows the quasiclassical continuation of (67) by joining it with the correct asymptotic behavior to take into account the curvature of the terms remote from the quasi-crossing region. The good agreement of theory with experiment makes it possible to reconstruct part of the unstable term.[81]

Up to now, we have been discussing the transition probability $\mathcal{P}(b)$. However, in order to predict the form of the differential cross-sections by Eq. (53), we must know the transition amplitudes $A_{nn_0}(b)$, not only in terms of moduli but also of phases. In the Landau-Zener approximation, in which the transitions in forward and backward flight R_p are independent, while the total probability is given by Eq. (60), the transition amplitudes $A_{nn_0}(b)$ can be written as:

$$\begin{aligned} A_{12} &= \sqrt{P(1-P)}\,[\exp\{i(2\bar{\delta}+\varphi+\gamma_1)\} + \exp\{i(2\bar{\delta}-\varphi+\gamma_2)\}], \\ A_{11} &= P\exp\{i(2\delta_1+\gamma_3)\} + (1-P)\exp\{i(2\delta_1-2\varphi+\gamma_4)\}; \end{aligned} \tag{68}$$

Here φ is determined by Eq. (61), and $\delta_i(b)$ (i = 1, 2) and $\bar{\delta}(b)$ are given by:

$$\delta_i(b) = \int_{R_i}^{\infty} k_i\,dR, \quad k_i = \frac{\sqrt{2\mu}}{\hbar}\left[E\left(1-\frac{b^2}{R^2}\right) - U_i^0(R)\right]^{1/2},$$
$$\bar{\delta} = \frac{1}{2}(\delta_1+\delta_2), \tag{69}$$

while the small phases γ_k are the additional phase shifts in the transition region that occur in the Landau-Zener formula (61).

Each term in (68) corresponds to a definite transition path. Eq. (68) implies that the differential cross-sections will arise from interference between the contributions from different trajectories of the process

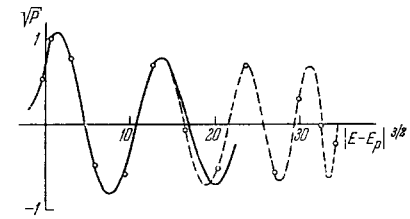

FIG. 18. Square root of the probability of predissociation of the O_2 molecule. [89] Circles: experimental data for different vibrational levels having energies measured from the quasi-crossing point. Solid curve: theoretical calculation.

corresponding to different values of b, but having the same scattering angle θ.[83-87] Here the phases of these contributions are determined by the classical actions along the corresponding trajectories with change of terms at the transition point R_p. Thus, the cross-sections for inelastic and elastic processes should oscillate in a certain angular range. Moreover, the properties of these oscillations at large energies (the relation of the period to the energy, etc.) should resemble the properties of charge-transfer oscillations (see Chap. 3).

Such oscillations of the cross-sections for inelastic processes (often called Stueckelberg oscillations) have actually been detected experimentally in many systems (He^+—He,[88] He^+—Ne,[36] Li^+—Li,[50] O^{++} + Ne,[89] He^+ + Ar,[90] Na^+ + Ne, K^+ + Ne[91]). Even earlier, the occurrence in scattering of an inelastic process has been indicated by anomalies observed in elastic scattering in He^+—He[92] or He^+—Ne, Ar[35] Figures 19 and 20 show typical structures of differential cross-sections of inelastic processes in cases of pseudo-crossing of terms. The most fully studied[36] process of inelastic scattering of He^+ by Ne will be discussed in detail below.

An important feature of the cross-sections of such processes is their threshold nature. In particular, the cross-section oscillates for values $\tau > \tau_{thr}$ greater than a certain threshold value τ_{thr}, but declines rather sharply at angles $\tau < \tau_{thr}$. Moreover, measurements of the cross-section at different angles give the constant value $\tau_{thr} = E\theta$ for the reduced threshold scattering angle. In exactly the same way, oscillations of elastic scattering (e.g., He^+ by Ne) caused by an inelastic process begin at a definite value $\tau = \tau_{thr}^{el}$, independent of the energy. (The values of τ_{thr} and of τ_{thr}^{el} do not coincide, since they roughly correspond to scattering in the differing potentials $U_1(R)$ and $[U_1(R) + U_2(R)]/2$.

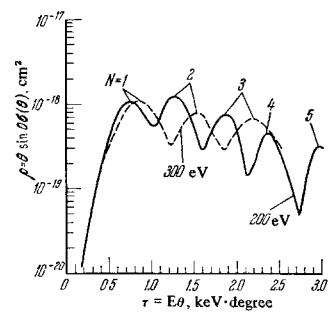

FIG. 19. Inelastic scattering cross-section of He^+ by He with formation of He (2^3 s). Cross-sections and angles are in terms of reduced variables.

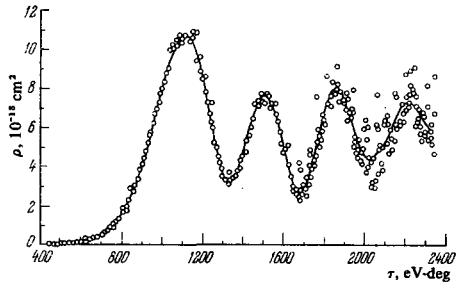

FIG. 20. Inelastic scattering cross-sections of He^+ by Ne at an energy of 71 eV with excitation of Ne to the $2p^5\,3s$ state. Cross-sections and angles are in terms of the reduced variables.

Thus, at large energies, the onset of the inelastic process corresponds to quite definite values (τ_{thr} or τ^{el}_{thr}) of the reduced angle, or, in view of the correspondence principle, to quite definite values of the impact parameter b. Thus, one can find the value $b_c = b_1^0|_{\tau=\tau_0^{elast}}$ from the scattering function for the first term $b_1^0(\tau)$, which is known from elastic-scattering data. Here the function $b_1^0(\tau)$ is monotonic for the repulsive potential U_1, so that larger b values correspond to smaller angles. It has been thought on these grounds[35,36] that the angle τ^{el}_{thr} that characterizes the onset (on the side of low τ) of oscillations in the elastic channel corresponds on the $b_1^0(\tau)$ curve to the maximum impact parameter for which the trajectory touches the crossing region. Hence it coincides with the radius R_p for crossing of the terms. However, we shall show below that this is not true, since scattering functions influenced by a combination of two potentials are not monotonic as $b_1^0(\tau)$ is. Hence, the value $b_c = b_1^0(\tau^{el}_{thr})$ does not coincide with R_p, although it is closely related.

The table, which is taken from[10], gives the values of b_c found in this way and the theoretically-predicted crossing distances R_p, together with the assumed symmetry of the intersecting terms for the different systems.

Following[93-95], we shall treat in more detail differential scattering cross-sections in the presence of an inelastic process. For simplicity, we shall restrict ourselves to the high-energy approximation, for which it is convenient to carry out the description in terms of the reduced angles τ and the cross-sections $\rho_{ij}(\tau, E)$.

The scattering amplitudes at the angle τ are expressed in terms of the transition amplitudes $A_{nn_0}(b)$ by using (51). Each term in the expressions (68) for A_{nn_0} corresponds to definite radial actions $\Delta_\nu(b)$: $\Delta^{\pm} = 2\delta \pm \varphi$ for inelastic scattering, and $2\delta_1$, $2\delta_1 - 2\varphi$ for elastic scattering. Hence, those impact parameters $b_\nu(\tau)$ will contribute to the scattering amplitudes at the given angle τ for which the total actions $S_\nu(b) = \Delta_\nu + 2b\tau/v^*$ are stationary in the variable b. Consequently, the deflection functions $b_\nu(\tau)$ or $\tau_\nu(b)$ that contribute to the process are:

$$\tau^{\pm}(b) = \bar{\tau}(b) \pm t(b), \tag{70}$$

$$\tau_1^0(b),\ \tau^{el}(b) = \tau_1^0(b) - 2t(b) \tag{71}$$

for inelastic and elastic scattering, respectively. Here $\tau_1^0(b)$ and $\bar{\tau}(b)$ are deflection functions in the potentials $U_1^0(R)$ and $\bar{U}(R) = (U_1^0 + U_2^0)/2$, while the function t(b) is determined in the high-energy approximation by the expression

$$t(b) = b\int_0^{\sqrt{R_0^2 - b^2}} \frac{1}{R}\frac{d\Delta U^0}{dR}\,dz,$$

$$\Delta U^0 = U_1^0 - U_2^0.$$

If we take into account the root-type behavior of t(b) near R_p:

$$t(b) = \Delta F\sqrt{2R_p(R_p - b)},\quad b \to R_p,$$

we can depict the form of the deflection functions that contribute to elastic and inelastic processes by referring to the deflection functions $\tau_1^0(b)$, $\tau_2^0(b)$ and $\bar{\tau}(b)$ in the potentials U_1^0, U_2^0, and $\bar{U}$ (Fig. 21). We see from Fig. 21 that two impact parameters contribute to interference in the cross-section ρ_{12} for angles τ larger than a certain threshold value τ_{thr} at which the function $\tau(b)$ passes through a minimum. Analogously, in elastic scattering, either two impact parameters contribute to interference in the cross-section when $\tau > \tau_p = \tau_1^0(R_p)$, or three impact parameters when $\tau_p < \tau < \tau^{el}_{thr}$. Here τ^{el}_{thr} is the threshold of the anomalies in the elastic cross-section, which differs from the threshold τ_{thr} of inelastic scattering, and is determined by the minimum on the $\tau^{el}(b)$ curve. When $\tau < \tau^{el}_{thr}$, we have unperturbed scattering by the first term.

System	τ^{el}_{thr}, eV·degree	b_c, atomic units	Signs of detection	Probable symmetry	R_p, atomic units
$He^+ - He$	1600	1,7	Oscillations	$^2\Sigma_g^+ - {}^2\Sigma_g^+$	1,5
$He^+ - Ne$	1950	1,9	Losses in the elastic channel	$^2\Sigma^+ - {}^2\Sigma$ *)	1,75
	2500—9500	1,4÷1,1		$^2\Sigma - {}^2\Sigma$ etc.	
$He^+ - Ar$	870	2,9	Oscillations	$^2\Sigma - {}^2\Sigma$ *)	
	1000—3000	2,4—1,9	Losses in the elastic channel	$^2\Sigma - {}^2\Sigma$ etc.	

*According to the conclusions of a new study. [36]

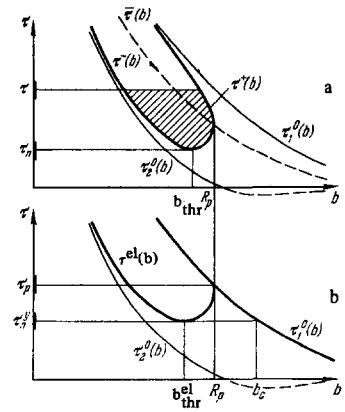

FIG. 21. Scattering in a system of two intersecting terms. a) Form of the deflection functions $\tau^{\pm}(b)$ heavy lines) that contribute to the inelastic process at angles above the threshold τ_{thr}. The functions $\tau_1^0(b)$, $\tau_2^0(b)$, and $\bar{\tau}(b)$ correspond to scattering in the potentials U_1, U_2, $\frac{1}{2}(U_1 + U_2)$; b) form of the deflection functions $\tau^{el}(b)$ and $\tau_1^0(b)$ that contribute to elastic scattering. The intervals marked out on the axis indicate the regions in which the quasi-classical description fails.

*The sign of the second term corresponds to repulsion.

Thus, the deflection functions are non-monotonic in nature when an inelastic process occurs. As was shown previously in[96], the same non-monotonic behavior occurs if there is any discontinuity of the potential, even in the absence of an actual inelastic process (e.g., in the case of a smoothed discontinuity of the adiabatic terms). However, when there is a non-monotonic deflection function, interference effects like rainbow scattering should be manifested,[27] and they will give rise to peculiarities in the differential cross-sections. The relation between the anomalies in the differential cross-sections observed in close collisions of ions and rainbow scattering has already been noted in[97], and it was confirmed by detailed analysis in[93]. They showed there that anomalies (peaks) will also characterize the total (elastic and inelastic) differential cross-sections.

One can derive very simple expressions for the cross sections at high energies for which the probability of an inelastic transition is small. In particular, if the energy exceeds the value E_{max} at which inelastic scattering has its maximum amplitude, then the motion of the system mainly follows the diabatic terms. Hence, the cross-section can be treated in the lowest-order perturbation theory of the interaction. Such a calculation gives the following quasiclassical expression for the inelastic cross-section when $\tau > \tau_{thr}$:

$$\rho_{12} = \left| \sqrt{\rho_1 (1 - P(b_1))}\, e^{iS_1} + i\sqrt{\rho_2 (1 - P(b_2))}\, e^{iS_2 - i\pi/2} \right|^2, \quad (72)$$

Here the reduced cross-sections

$$\rho_k(\tau) = \frac{1}{2}\frac{db_k^2}{d\ln\tau}$$

correspond to the branches $b_1(\tau)$ and $b_2(\tau)$ ($\tau > \tau_{thr}$), which are inverse functions of $\tau^{\pm}(b)$; $P(b)$ is the ordinary transition probability of (58) for small V_{12};

$$1 - P(b) = \frac{2\pi V_{12}^2}{\hbar \Delta F v_R}, \quad v_R = v\sqrt{1 - \frac{b^2}{R^2}}.$$

The phase difference of the two terms of (72) that determine the experimental phase $2\pi N(\tau, E)$ of the oscillations of the cross-section ρ_{12} is

$$2\pi N(\tau, E) = S_2 - S_1 - \frac{\pi}{2} = \frac{2}{v}\int_{\tau_{thr}}^{\tau} \Delta b(\tau)\, d\tau, \quad \Delta b = b_1 - b_2, \quad (73)$$

That is, it is determined by the area of the cross-hatched region in the diagram. At angles near the threshold value, the quasiclassical expression (72) is inapplicable, and it must be replaced with the quantum expression. In full analogy with the rainbow phenomenon (see[39]), the cross-section ρ_{12} is expressed as follows in the vicinity of τ_{thr} in terms of an Airy function:[93,94,98]

$$\rho(\tau, E) = \frac{8\pi V_{12}^2 \tau b_{thr} R_p}{\Delta F \sqrt{R_p^2 - b_{thr}^2}} v^{-4/3} \chi^{-2} \Phi^2(-2\Delta\tau v^{-2/3}\chi), \quad (74)$$

$$\Delta\tau = \tau - \tau_{thr}, \quad \chi = \left(\frac{d^2\tau}{db^2}\Big|_{b_{thr}}\right)^{-1/3}.$$

For elastic scattering, the quasiclassical expressions for the cross-section corresponding to the branches τ_1^0 and τ^{elast} of Fig. 21 are given in[93,94]. In the neighborhoods of the angles τ_{thr}^{elast} and τ_p (see Fig. 21) where the different branches of the scattering function merge, the quasiclassical description is inapplicable. In these regions, calculation leads to the quantum formulas for the cross-section (they express ρ_{11} in terms of an Airy function when $\tau \sim \tau_{thr}^{el}$, and in terms of a parabolic-cylinder function when $\tau \sim \tau_p$) correctly merge with the quasiclassical expressions outside these regions.

We note one important fact. The anomalies in the elastic channel caused by the inelastic process begin on the small-angle side at $\tau \sim \tau_{thr}^{el}$ (see Fig. 21b). Here the value $b_c = b_1^0(\tau_{thr}^{el})$ that corresponds to this τ is identified with the crossing radius R_p to a rough approximation[35,36] but actually does not coincide with it: $b_c > R_p$. Perhaps this explains the reason why the experimental values of b_c found from the onset of anomalies in the elastic channel are higher than the theoretical values of R_p (see the table above).

Thus one can gain information from the oscillations of the inelastic and elastic cross-sections on the corresponding scattering functions $\tau^{\pm}(b)$ and $\tau^{elast}(b)$, which are defined by Eqs. (70) and (71), and then one can find the parameters of the ground term $U_1^0(R)$ and the excited term $U_2^0(R)$ of the system.

Now we shall take up an analysis of inelastic scattering in the system He^+—Ne, which has been most fully studied experimentally. Figure 20 gives the inelastic cross-section for excitation of the $2p^5 3s$ configuration of the Ne atom in collisions with He^+ ions, as measured in[36]. In addition to the rapid Stueckelberg oscillations visible in Fig. 20, the cross-section $\rho_{12}(\tau, E)$ (both in amplitude of the first peak and in other characteristics) shows a slow modulation. The authors of[36] ascribe it to the existence of a second dissociation channel (Ne^+—He(1s2s) of the excited state that arises in the quasi-crossing region. However, we shall restrict ourselves here to discussing only the properties of the rapid (Stueckelberg) oscillations, and in particular, to quantum effects in inelastic scattering.

Beginning with about the second period of oscillations and beyond, in accord with the quasiclassical formulas (72) and (73), the experimental phase of the oscillations $2\pi N(\tau, E)$ ($N = 1, 2, \ldots$ at the peaks, and $N = 3/2, 5/2, \ldots$ at the minima of $\rho_{12}(\tau)$) proves to be proportional to $E^{-1/2}$, so that the quantity

$$\Delta b = \pi v \frac{\partial N(\tau, E)}{\partial \tau} \approx E^{1/2}\frac{\partial N}{\partial \tau} = \text{const} \quad (75)$$

does not depend on E, and is approximately equal to 0.36 atomic units. However, as $\tau \to \tau_{thr}$, the quantity

$$E^{1/2}\frac{\partial N}{\partial \tau}\Big|_{\tau=\tau_N} \approx \frac{E^{1/2}}{\tau_2 - \tau_1} \approx E^{1/6} \quad (76)$$

(τ_N is the location of the Nth peak) depends on the energy. In fact, if at large τ ($N \leq 2$) the period of the oscillations in τ, which is equal to $(dN/d\tau)^{-1}_{\tau_N}$, is proportional to $E^{1/2}$, then the period $(\tau_2 - \tau_1)$ and the half-period $(\tau_{3/2} - \tau_1)$ that follow first after the threshold of the oscillations of the cross-section should be linear functions of $E^{1/3}$, according to (74), with a ratio of slopes of 1.69, as is observed experimentally (Fig. 22). Analogously, the quantity in (76) as a function of the energy should be proportional to $E^{1/6}$, whereas the quasiclassical theory makes this quantity independent of the energy. The agreement of the theoretical relation with experiment confirms the necessity of a quantum analysis (in distinction from the quasiclassical analysis) of scattering near the threshold of an inelastic process.

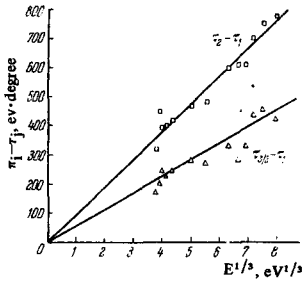

FIG. 22. Relation of the sizes of the first period $\tau_2 - \tau_1$ and the half-period $\tau_{3/2} - \tau_1$ in the oscillations of the inelastic scattering cross-section of He^+ by Ne to the 1/3 power of the energy. The ratio of slopes 1.69 of the straight lines that approximate the experimental points corresponds to the theoretical value.

An analogous application of the analytic expressions[94] to handle the experimental data on elastic scattering of He^+ by Ne near the threshold of the anomalies is complicated by the fact that in this system the regions $\tau_p \sim \tau_{thr}^{el}$ and $\tau \sim \tau_{thr}^{el}$, in which the quantum description is necessary, prove to be very close together. In such a case, one must find the cross-sections numerically. Figure 23 gives the result of such a calculation[95] of the elastic cross-section of the system $He^+ + Ne$. The theoretical and experimental curves show excellent agreement.

Up to now, we have been treating inelastic processes arising from quasi-crossing of terms. However, there are a large number of inelastic processes that cannot be described by a quasi-crossing model. For example, these include inelastic transitions having a small resonance defect. We cannot take up in detail the other types of non-adiabatic transitions and models to describe them,[14,15] as well as the numerous experiments concerned with these processes.

Analogously, we cannot throw any light on the entire field of phenomena involving highly-excited atomic states. The point is that we have been restricting ourselves up to now in the discussion to examples of inelastic processes having a relatively low level of excitation that involves only the outer shells of the atoms. However, high excitations of atoms that involve the inner shells are also of great interest. Such processes have been widely studied, mainly in the work of Afrosimov, Federenko, et al.[99,97] and of Everhart and his associates,[100] where they measured by coincidence techniques both the energy losses and the charge states of particles that had undergone close collisions. Here, both the energy losses and the number of emitted electrons increase sharply at quite definite critical distances ($R \approx 0.5$, 0.2 atomic units), which correspond to overlap of the inner shells of the atoms. It turns out that these results can be understood[101,20] by the same methods as the processes of excitation of the outer shells, in terms of quasi-crossing of the molecular levels of the inner electrons. This possibility arises from the fact that the dimensions of the transition region ΔR remains, as before, less than the characteristic dimensions R_1 of the given atomic shell, in spite of the increase in both the interactions and the characteristic energy ranges. The phenomena observed here are accompanied by emission of an inner electron, with subsequent Auger transition with emission of several electrons from the outer shell. Detailed description of this field of phenomena is undoubtedly worthy of an independent review.

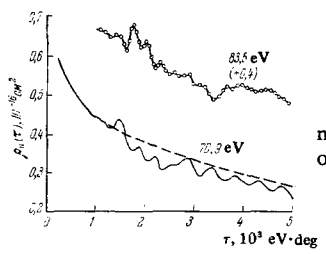

FIG. 23. Theoretical and experimental elastic scattering cross-sections of He^+ by Ne. [95]

In conclusion, we shall mention another phase-interference effect, which is manifested in the fact that the total (rather than only differential) cross-sections for excitation and charge transfer show a complex oscillatory structure in many systems: $He^+ - He$[102] $Na^+ - Ne$,[103] $Zn^+ - Cd$.[104] One of the possible models[105,106] of this effect assumes that the excited term is split (e.g., into spin states). Then, in addition to the region (R_p) of transition from the ground term to the excited multiplet, there is a region (R_1) in which transitions occur within a group of close excited levels. Here the total cross-section for excitation of each individual line of the multiplet will oscillate with a phase that depends on the splitting of the terms and the location of the regions of R_p and R_1. A detailed interpretation of the observed oscillations of the cross-sections will permit us in the future to elucidate the terms of ion-atom systems and to understand the mechanisms of various excitation processes.

[1] V. de Alfaro and T. Regge, Potential Scattering, North-Holland, Amsterdam, 1965 (Russ. Transl., M., Mir, 1966).

[2] A. I. Baz', Ya. B. Zel'dovich, and A. M. Perelomov, Rasseyanie, reaktsii i raspady v nerelyativistskoĭ kvantovoĭ mekhanike (Scattering, Reactions and Decay in Nonrelativistic Quantum Mechanics), M., Nauka, 1966 (Engl. Transl., Israel Program for Scientific Translations, Jerusalem, 1969).

[3] M. L. Goldberger and K. M. Watson, Collision Theory, Wiley, New York, 1964 (Russ. Transl., M., Mir, 1967).

[4] T.-Y. Wu and T. Ohmura, Quantum Theory of Scattering, Prentice-Hall, Englewood Cliffs, N. J., 1962 (Russ. Trans., M., Nauka, 1969).

[5] B. M. Smirnov, Atomnye stolknoveniya i élementarnye protsessy v plazme (Atomic Collisions and Elementary Processes in a Plasma), M., Atomizdat, 1968.

[6] R. G. Newton, Scattering Theory of Waves and Particles, McGraw-Hill, New York, 1966 (Russ. Transl., M., Mir, 1969).

[7] H. Pauly and J. P. Toennies, Adv. Atom. Mol. Phys. 1, 195 (1965).

[8] D. Allab, M. Barat, and J. Baudon, J. de Phys. 29, 111 (1968).

[9] V. B. Leonas, Usp. Fiz. Nauk 82, 287 (1964) [Sov. Phys.-Uspekhi 7, 121 (1964)].

[10] F. T. Smith, Proceedings of the International Conference on Atomic Physics, New York, 1968.

[11] F. T. Smith, Proceedings of the International Symposium on Physics of One- and Two-Electron Atoms, North-Holland, 1969.

[12] Yu. N. Demkov, Sbornik lektsiĭ 1-ĭ Vsesoyuznoĭ shkoly po êlektronnym i atomnym stolknoveniyam (Collected Lectures of the First All-Union School of Electronic and Atomic Collisions), Khar'kov, 1969.
[13] N. F. Mott and H. S. W. Massey, The Theory of Atomic Collisions, 3rd Edn., Clarendon Press, Oxford, 1965 (Russ. Transl., M., Mir, 1969).
[14] E. E. Nikitin, Adv. Quant. Chem. 5, 135 (1970).
[15] E. E. Nikitin, Chemische Elementarprozesse, Springer-Verlag, 1968.
[16] W. Lichten, Phys. Rev. 131, 229 (1963).
[17] F. T. Smith, Phys. Rev. 179, 111 (1969).
[18] D. R. Bates and R. McCarroll, Proc. Roy. Soc. A245, 175 (1958).
[19] D. R. Bates, ibid. A245, 299 (1958).
[20] W. Lichten, Phys. Rev. 164, 131 (1967).
[21] D. R. Bates, Atomic and Molecular Processes, Academic Press, New York, 1962 (Russ. Transl., M., Mir, 1964).
[22] L. D. Landau and E. M. Lifshitz, Kvantovaya mekhanika (Quantum Mechanics), M., Fizmatgiz, 1963 (Engl. Transl., Addison-Wesley, Reading, Mass., 1965).
[23] E. C. G. Stueckelberg, Helv. Phys. Acta 5, 369 (1932).
[24] D. R. Bates and A. R. Holt, Proc. Roy. Soc. A292, 168 (1966).
[25] L. Wilets and S. J. Wallace, Phys. Rev. 169, 84 (1968).
[26] J. C. Y. Chen and K. M. Watson, ibid. 174, 152 (1968).
[27] K. W. Ford and I. A. Wheeler, Ann. Phys. 7, 259 (1959).
[28] R. B. Bernstein, in Atomic Collision Processes, Ed. M. R. C. McDowell, North-Holland, Amsterdam, 1964, p. 895.
[29] R. B. Bernstein, in Issledovaniya s molekulyarnymi puchkami (Studies with Molecular Beams), M., Mir, 1969, p. 88.
[30] W. Neumann and H. Pauly, J. Chem. Phys. 52, 2548 (1970).
[31] F. C. Hoyt, Phys. Rev. 55, 664 (1939).
[32] O. B. Firsov, Zh. Eksp. Teor. Fiz. 24, 279 (1953).
[33] C. Lehmann and G. Leibfried, Z. Phys. 172, 465 (1962).
[34] F. T. Smith, R. P. Marchi, and K. G. Dedrick, Phys. Rev. 150, 79 (1966).
[35] F. T. Smith, R. P. Marchi, W. Aberth, D. C. Lorents, and O. Heinz, ibid. 161, 31 (1967).
[36] D. Coffey, Jr., D. C. Lorents, and F. T. Smith, ibid. 187, 201 (1969).
[37] F. J. Zehr and H. W. Berry, Phys. Rev. 159, 13 (1967).
[38] R. E. Olson, F. T. Smith, and C. R. Muller, ibid. A1, 27 (1970).
[39] M. V. Berry, Proc. Phys. Soc. 89, 479 (1966).
[40] R. B. Bernstein, J. Chem. Phys. 38, 2599 (1963).
[41] U. Buck and H. Pauly, Z. Naturforsch. 23A, 475 (1968).
[42] F. M. Mott, Proc. Roy. Soc. A126, 259 (1930).
[43] P. E. Siska, J. M. Parson, T. P. Schafer, F. P. Tully, Y. C. Wong, and Y. T. Lee, Phys. Rev. Lett. 25, 271 (1970).
[44] G. J. Lockwood and E. Everhart, Phys. Rev. 125, 567 (1962).
[45] H. F. Helbig and E. Everhart, Phys. Rev. 140, A715 (1965).
[46] F. P. Ziemba and E. Everhart, Phys. Rev. Lett. 2, 229 (1959).
[47] G. J. Lockwood, H. F. Helbig, and E. Everhart, Phys. Rev. 132, 2078 (1963).
[48] E. Everhart, Phys. Rev. 132, 2083 (1963).
[49] D. C. Lorents and W. Aberth, Phys. Rev. 139, A1017 (1965).
[50] W. Aberth, O. Bernardini, D. Coffey, Jr., D. C. Lorents, and R. E. Olson, Phys. Rev. Lett. 24, 345 (1970).
[51] P. R. Jones, T. L. Batra, and H. A. Ranga, ibid. 17, 281 (1966).
[52] F. J. Smith, Phys. Lett. 20, 271 (1966).
[53] J. M. Peek, T. A. Green, J. Perel, and H. H. Michels, Phys. Rev. Lett. 20, 1419 (1968).
[54] B. M. Smirnov, Zh. Eksp. Teor. Fiz. 47, 518 (1964) [Sov. Phys.-JETP 20, 345 (1965)].
[55] J. Perel, R. H. Vernon, and H. L. Daley, Phys. Rev. 138, A937 (1965).
[56] R. E. Olson, Phys. Rev. 187, 153 (1969).
[57] D. R. Bates, K. Ledsham, and A. L. Stewart, Phil. Trans. Roy. Soc. A246, 215 (1953).
[58] F. J. Smith, Proc. Phys. Soc. 84, 889 (1964); Phys. Lett. 10, 290 (1964).
[59] F. T. Smith, Bull. Amer. Chem. Soc. 9, 411 (1963).
[60] H. S. W. Massey and R. A. Smith, Proc. Roy. Soc. A142, 142 (1933).
[61] R. P. Marchi and F. T. Smith, Phys. Rev. 139, A1025 (1965).
[62] Yu. N. Demkov and Yu. E. Murakhver, Zh. Eksp. Teor. Fiz. 49, 635 (1965). [Sov. Phys.-JETP 22, 441 (1966)].
[63] W. Aberth, D. C. Lorents, R. P. Marchi, and F. T. Smith, Phys. Rev. Lett. 14, 776 (1965).
[64] D. R. Bates and D. A. Williams, Proc. Phys. Soc. 83, 425 (1964).
[65] B. M. Smirnov, Optika i Spektroskopiya 17, 504 (1964) [Optics and Spectroscopy 17, 273 (1964)].
[66] Yu. N. Demkov, G. V. Dubrovskiĭ, and A. M. Ermolaev, Abstracts of Papers to the 5th International Conference on the Physics of Electronic and Atomic Collisions, Leningrad, 1967, p. 186.
[67] L. Wilets and D. F. Gallaher, Phys. Rev. 147, 13 (1966).
[68] D. F. Gallaher and L. Wilets, Phys. Rev. 169, 139 (1968).
[69] J. E. Bayfield, Phys. Rev. Lett. 25, 1 (1970).
[70] R. N. Varney, Phys. Rev. 47, 483 (1935).
[71] D. R. Bates and D. F. Grothers, Proc. Roy. Soc. A315, 465 (1970).
[72] L. Landau, Phys. Z. Sowjetunion 1, 88 (1932); 2, 46 (1932).
[73] C. Zener, Proc. Roy. Soc. A137, 696 (1932).
[74] S. V. Bobashev, V. B. Matveev, and V. A. Ankudinov, ZhETF Pis. Red. 9, 344 (1969) [JETP Lett. 9, 201 (1969)].
[75] V. B. Matveev, Candidate's Dissertation (FTI, Leningrad, 1970).
[76] E. E. Nikitin, Optika i Spektroskopiya 11, 452 (1961) [Optics and Spectroscopy 11, 246 (1961)].
[77] M. Ya. Ovchinnikova, ibid. 17, 821 (1964) [Optics and Spectroscopy 17, 447 (1964)].

[78] V. K. Bykhovskiĭ, E. E. Nikitin, and M. Ya. Ovchinnikova, Zh. Eksp. Teor. Fiz. 47, 750 (1964) [Sov. Phys.-JETP 20, 500 (1965)].
[79] Yu. S. Sayasov, Zh. Eksp. Teor. Fiz. 46, 560 (1964) [Sov. Phys-JETP 19, 382 (1964)]; also see[78].
[80] G. V. Dubrovskiĭ, ibid. 46, 863 (1964) [Sov. Phys.-JETP 19, 591 (1964)].
[81] M. S. Child, J. Mol. Spectr. 33, 487 (1964).
[82] J. N. Murrell and J. M. Taylor, Mol. Phys. 16, 609 (1969).
[83] L. P. Kotova, Zh. Eksp. Teor. Fiz. 55, 1375 (1968) [Sov. Phys.-JETP 28, 719 (1969)].
[84] T. A. Green and R. E. Johnson, Phys. Rev. 152, 9 (1966).
[85] T. A. Green, Phys. Rev. 152, 18 (1966).
[86] M. Matsusawa, J. Phys. Soc. Japan 25, 1153 (1968).
[87] F. T. Smith, in Atomic Collision Processes, Lectures in Theoretical Physics, Vol. XI-C, Ed. S. Geltman, New York, 1969.
[88] D. C. Lorentz, W. Aberth, and V. W. Hesterman, Phys. Rev. Lett. 17, 849 (1966).
[89] G. D. Alam, D. K. Bohme, J. B. Haster, and P. P. Ong, see[66].
[90] F. T. Smith, H. H. Fleischmann, and R. A. Young, Phys. Rev. 2A, 379 (1970).
[91] V. V. Arosimov, Yu. S. Gordeev, V. M. Lavrov, and V. K. Nikulin, Abstract of Paper VII ICPEAC.
[92] F. T. Smith, D. C. Lorents, W. Aberth, and R. P. Marchi, Phys. Rev. Lett. 15, 742 (1965).
[93] V. V. Afrosimov, Yu. S. Gordeev, V. K. Nikulin, A. M. Polyanskii, and A. P. Shchergin, see[9].
[94] L. P. Kotova and M. Ya. Ovchinnikova, Zh. Eksp. Teor. Fiz. 60, 2026 (1971) [Sov. Phys.-JETP 33, 1092 (1971)].
[95] R. E. Olson and F. T. Smith, Phys. Rev. A3, 1607 (1971).
[96] R. P. Marchi, Phys. Rev. 183, 185 (1969).
[97] V. V. Afrosimov, in A Survey of Phenomena in Ionized Gases, International Atomic Energy Agency, Vienna, 1961, p. 91.
[98] M. Ya. Ovchinnikova, Zh. Eksp. Teor. Fiz. 59, 1795 (1970) [Sov. Phys.-JETP 32, 974 (1971)].
[99] V. V. Afrosimov, Yu. S. Gordeev, M. N. Panov, and N. V. Fedorenko, Zh. Tekh. Fiz. 34, 1613, 1637 (1964) [Sov. Phys.-Tech. Phys. 9, 1248, 1265 (1965)].
[100] Q. C. Kessel and E. Everhart, Phys. Rev. 146, 16 (1966).
[101] U. Fano and W. Lichten, Phys. Rev. Lett. 14, 627 (1965).
[102] S. H. Dworetsky and R. Novick, Phys. Rev. Lett. 23, 1484 (1969).
[103] S. V. Bobashev, ZhETF Pis. Red. 11, 389 (1970) [JETP Lett. 11, 260 (1970)].
[104] O. B. Shpenik, I. P. Zapesochnyĭ, and A. N. Zavilopulo, Zh. Eksp. Teor. Fiz. 60, 513 (1970) [Sov. Phys.-JETP 33, 277 (1971)].
[105] H. Rosenthal and H. M. Foley, Phys. Rev. Lett. 23, 1480 (1969).
[106] V. A. Ankudinov, S. V. Bobashev, and V. I. Perel', Zh. Eksp. Teor. Fiz. 60, 906 (1971) [Sov. Phys.-JETP 33, 490 (1971)].
[107] A. Z. Devdariani and S. V. Bobashev, ibid. 60, 485 (1971) [Sov. Phys.-JETP 33, 260 (1971)].
[108] J. M. Parson, T. P. Schafer, F. P. Tully, P. E. Siska, Y. C. Wong, and Y. T. Lee, J. Chem. Phys. 53, 2123 (1970).

Translated by M. V. King